The Company of **Biologists**

RESEARCH ARTICLE

RH17 restricts reproductive fate and represses autonomous seed coat development in sexual *Arabidopsis*

Ron Eric Stein[1,§], Berit Helge Nauerth[1,§], Laura Binmöller[1], Luise Zühl[1,*], Anna Loreth[1], Maximilian Reinert[1], David Ibberson[2] and Anja Schmidt[1,‡,¶]

ABSTRACT

Plant sexual and asexual reproduction through seeds (apomixis) is tightly controlled by complex gene regulatory programs, which are not yet fully understood. Recent findings suggest that RNA helicases are required for plant germline development. This resembles their crucial roles in animals, where they are involved in controlling gene activity and the maintenance of genome integrity. Here, we identified previously unknown roles of *Arabidopsis RH17* during reproductive development. Interestingly, RH17 is involved in repression of reproductive fate and of elements of seed development in the absence of fertilization. In lines carrying a mutant *rh17* allele, development of supernumerary reproductive cell lineages in the female flower tissues (ovules) was observed, occasionally leading to formation of two embryos per seed. Furthermore, seed coat, and putatively also endosperm development, frequently initiated autonomously. Such induction of several features phenocopying distinct elements of apomixis by a single mutation is unusual and suggests that RH17 acts in regulatory control of plant reproductive development. Furthermore, an in-depth understanding of its action might be of use for agricultural applications.

KEY WORDS: *Arabidopsis*, Apomixis, Autonomous seed coat, Endosperm, RNA helicase, Polyembryony

INTRODUCTION

In higher plants, the life cycle alternates between two distinct generations, with the sporophyte as the dominant generation and the gametophytes being reduced to a few cells only. The transitions between generations are of crucial importance and need to be thoroughly regulated. The formation of the female and male gametophytic lineages takes place in specialized reproductive organs of the flowers, which are the ovules and the anthers, respectively. In sexual plants, a single sporophytic cell typically specifies in the subepidermal ovule tissues to give rise to the functional megaspore (FMS) as the first cell of the female

gametophytic lineage (Schmidt et al., 2015). This megaspore mother cell (MMC) is committed to a meiotic fate. Three of the four meiotically derived megaspores undergo apoptosis. The surviving FMS subsequently goes through three rounds of mitosis in a syncytium followed by cellularization. In *Arabidopsis*, like in the majority of angiosperms, a Polygonum-type mature gametophyte is formed comprising four specialized cell types (Schmid et al., 2015). These are the two female gametes (egg and central cell), two synergids, which are important for pollen tube attraction and double fertilization, and three antipodal cells. Similarly, the male reproductive lineage initiates development with the selection of a single sporophytic cell in the anther, termed the pollen mother cell (PMC) (Borg et al., 2009). Four microspores are derived from meiosis of the PMC. Two subsequent mitotic divisions lead to the formation of two sperm cells engulfed in a vegetative cell. In sexual plants, double fertilization of the female gametes with one sperm cell each initiates the coordinated development of the embryo, endosperm and seed coat. The zygote resulting from the fertilized egg cell first elongates before an apical cell and a basal cell are formed through an asymmetric division (Hove et al., 2015). The apical cell then gives rise to most of the embryo with the exception of its basal end; the basal cell differentiates to form the suspensor. Embryo development thereby proceeds through defined developmental stages, with the formation of a globular embryo, which subsequently traverses through heart and torpedo stages to give rise ultimately to the mature embryo (Hove et al., 2015).

In addition to sexual reproduction, asexual reproduction through seeds (apomixis) is also common in plants. From an evolutionary point of view, the co-existence of sexual reproduction and apomixis is of great interest. Apomixis has classically been regarded as a dead end of evolution. However, alternative hypotheses have recently emerged, including the possibility of a switch of the mode of reproduction in response to environmental stress (Albertini et al., 2019; Carman et al., 2019; Schmidt, 2020). Furthermore, apomixis has great potential for applications in agriculture, as it leads to formation of offspring that is genetically identical to the mother plant (Barcaccia and Albertini, 2013; Conner and Ozias-Akins, 2017). Engineering of apomixis in crops would therefore enable the fixation of superior genotypes. However, a precise understanding of the molecular programs governing plant reproduction will be required to achieve this.

Developmentally, different types of apomixis are recognized. First, sporophytic and gametophytic apomixis are distinguished based on the origin of the embryo (Bicknell and Koltunow, 2004; Koltunow and Grossniklaus, 2003). In gametophytic apomicts, the clonal embryo is derived from the egg cell. During diplospory, an apomictic initial cell forms instead of the MMC and alters meiosis to give rise to the gametophytic cell lineage. In contrast, during apospory an additional sporophytic cell, the aposporous initial cell (AIC), specifies adjacent to the MMC. It adopts a gametophytic

[1]Centre for Organismal Studies Heidelberg, Department of Biodiversity and Plant Systematics, Heidelberg University, Im Neuenheimer Feld 345, D-69120 Heidelberg, Germany. [2]Deep Sequencing Core Facility, CellNetworks Excellence Cluster, Heidelberg University, Im Neuenheimer Feld 267, D-69120, Heidelberg, Germany.
*Present address: Max Planck Institute for Plant Breeding Research, Department of Comparative Development and Genetics, Carl-von-Linné-Weg 10, D-50829 Cologne, Germany. ‡Present address: Institute of Biology, University of Hohenheim, Garbenstraße 30, Stuttgart D-70599 Germany.
§These authors contributed equally to this work

¶Author for correspondence (anja.schmidt@alumni.uni-heidelberg.de)

R.E.S., 0000-0002-7691-1295; M.R., 0000-0003-0992-0340; D.I., 0000-0003-1474-3158; A.S., 0000-0002-3276-3243

DEVELOPMENT

1

fate without undergoing meiosis. In both cases, after gametogenesis the egg cell gives rise to the embryo in the absence of fertilization (parthenogenesis). In contrast, fertilization is required for endosperm formation in the majority of apomicts, but autonomous endosperm development also occurs. Unlike in gametophytic apomixis, in sporophytic apomicts asexual embryos form directly from sporophytic cells of the ovule tissues enclosing the sexual gametophyte. This frequently leads to polyembryony. Furthermore, apospory occasionally leads to polyembryony resulting from the formation of both the sexual and the apomictic reproductive lineages, derived from the MMC and the AIC, respectively, in the same ovule (Schmidt, 2020).

Formation of additional embryos per seed can be observed during sexual reproduction in some taxa. In gymnosperms, as well as in *Orchidaceae* and *Poaceae*, they derive from irregular divisions of the developing embryo, typically from the suspensor (Kishore, 2014). Alternatively, cell type mis-specification during gametogenesis can give rise to a second egg cell, mostly instead of one synergid cell, as has been described for French bean (Kishore, 2014). In most sexual species, including *Arabidopsis*, polyembryony is very rare. Nevertheless, in *twin* mutants two to three embryos per seed originate from the proliferation of suspensor cells (Vernon and Meinke, 1994), whereas in lines lacking the function of *ALTERED MERISTEM PROGRAM 1* supernumerary egg cells are formed (Kong et al., 2015). In addition, formation of two embryos per seed occurs at low frequencies in septuple mutants deficient in all members of the gene family encoding for KIP-related proteins (ICK/KRP) (Cao et al., 2018). KRP genes act redundantly during germline formation and are involved in controlling the entry into meiosis (Zhao et al., 2017). Therefore, the embryos likely originate from egg cells formed in supernumerary meiotically derived gametophytes. In contrast, polyembryony from apospory-like development has thus far not been described for *Arabidopsis*.

Nevertheless, components of apomixis have been observed in sexual species (Schmidt et al., 2015), involving elements of autonomous seed development. During sexual reproduction, both endosperm and seed coat development typically stay repressed in the absence of fertilization, a process governed by the activity of Polycomb group proteins (Figueiredo and Köhler, 2018). These act in multimeric complexes to repress the activity of target genes by introducing histone methylation marks (Figueiredo and Köhler, 2018; Mozgova et al., 2015). Interestingly, Polycomb repressive complex 2 (PRC2) also represses genes involved in auxin biosynthesis, and auxin is sufficient to induce autonomous development of endosperm and seed coat (parthenocarpy) (Figueiredo et al., 2016; Figueiredo and Köhler, 2018). Moreover, features of apospory or diplospory have been described for certain mutants of core meiotic genes or genes involved in epigenetic regulatory pathways, which control gene expression based on DNA methylation or the activity of small RNAs (Hand and Koltunow, 2014; Lora et al., 2019; Nakajima, 2018; Schmidt et al., 2015). Phenotypes closely resembling apospory have also been reported for lines carrying a mutant allele of the RNA helicase *MNEME* (*MEM*) (Schmidt et al., 2011).

RNA helicases are becoming increasingly recognized as crucial for germline development (Schmidt, 2020). They are required for various aspects of RNA metabolism, including RNA stabilization, degradation and translation, and are involved in small RNA pathways (Owttrim, 2013). In addition, RNA helicases, together with other RNA-binding proteins, are crucial components of ribonucleoprotein particles (RNPs) (Martin et al., 2013). Ribosome assembly and activity has classically been regarded as constitutive in cells. Nevertheless, increasing evidence suggests that in germlines regulatory mechanisms involving ribosomes play roles in controlling gene activity and developmental processes (Schmidt, 2020). In *Arabidopsis*, 58 DEAD-box RNA helicase (RH) proteins are represented (Mingam et al., 2004), 24 of which are putative ribosome biogenesis factors (Liu and Imai, 2018), but only a few of them have been described to date (Chi et al., 2012; Hsu et al., 2014; Lee et al., 2013; Nishimura et al., 2010; Paieri et al., 2018). *RH3* and *RH22* are active in chloroplasts and are among the 510 *EMBRYO DEFECTIVE* genes recognized to date (Meinke, 2020). The importance of gametogenesis has only been reported for RH36 (SLOW WALKER 3), which is involved in 18S-preRNA processing (Huang et al., 2010; Liu et al., 2010). Interestingly, homology with the yeast protein Dbp7p and investigations on the rice homolog *OsRH17* suggest that *Arabidopsis* RH17 could potentially act in ribosome biogenesis (Liu and Imai, 2018; Xu et al., 2015). This identifies RH17 as a promising candidate for controlling aspects of reproductive development.

To study the potential roles of RH17 in reproduction, we used independent *Arabidopsis* lines carrying mutant alleles. Homozygous mutants were not recovered, in line with an embryo lethal and partially penetrant male gametophytic defect. Consistently, defects during seed development were observed, including embryo developmental arrest and over-proliferation of embryos. Interestingly, two embryos per seed formed at low frequencies. These likely derived from a second gametophyte originating from an AIC-like cell specifying adjacent to the MMC in the same ovule. In addition, we identified that in our lines carrying mutant alleles seed coat and likely also endosperm development initiated in the absence of fertilization at certain frequencies. In agreement with this, RNA sequencing (RNA-Seq) on ovules collected 3 days after emasculation (DAE) from a line carrying a mutant allele of *RH17* confirmed an enrichment of genes involved in seed coat development in the set of differentially expressed genes (DEGs) compared with wild type, in addition to genes involved in stress response and hormonal pathways. Taken together, our results show that mutant alleles of *RH17* lead to phenotypes resembling elements of apomixis, which could link ribosomal pathways, stress response and hormonal pathways to the regulation of reproductive development.

RESULTS
RHs are broadly active in reproductive tissues
Increasing evidence suggests that certain RHs are involved in ribosome assembly and turnover, thereby contributing to the control of gene activity (Liu and Imai, 2018; Schmidt, 2020). Interestingly, *Arabidopsis* RHs likely representing ribosome-binding factors are broadly expressed in reproductive tissues (Fig. S1). Based on its expression and localization of the protein to the nucleus (Fig. S1A-G) (Kiefer et al., 2020; Nguyen et al., 2018), we identified *RH17* as a candidate for regulation of aspects of reproductive development. *RH17* is present in a variety of cell and tissue types, including female reproductive tissues and germline cells, particularly the MMC and the surrounding nucellus, ovules at early and late stages of gametogenesis, and the female gametes (Fig. S1A, B). During male germline development, *RH17* is expressed in meiocytes, in uninucleate microspores and bicellular pollen, unlike in mature pollen or sperm (Fig. S1A,B). Following double fertilization, *RH17* is present at early stages of seed development in the embryo, endosperm and seed coat, predominantly at the preglobular stage of embryogenesis. In contrast to sexual *Arabidopsis*, expression of the *RH17* homolog was not observed in the apomictic initial cell or in

Table 1. Transmission efficiencies of mutant alleles

	Number of heterozygous offspring observed	Number of wild-type offspring observed	Number of heterozygous offspring expected	Number of wild-type offspring expected	Total	χ^2	Transmission efficiencies (%)
rh17-1/RH17×RH17/RH17	680	625	652.5	652.5	1305	2.318	109
RH17/RH17×rh17-1/RH17	362	428	395	395	790	5.514	85
rh17-2/RH17×RH17/RH17	42	39	40.5	40.5	81	0.111	108
RH17/RH17×rh17-2/RH17	42	59	50.1	50.1	101	2.861	71

Analysis was carried out by scoring resistance to sulfadiazine for *rh17-1/RH17* and PCR-based genotyping for *rh17-2/RH17* after reciprocal crosses to the wild type. $\chi^2 > \chi^2_{(0.05)} = 3.58$ corresponds to a significant deviation from the expected segregation rate.

cells of the mature gametophyte in the apomict *Boechera gunnisoniana* (Fig. S1B).

Mutant alleles of *RH17* cause defects during reproductive development

To gain insights into the functional roles of *RH17* in *Arabidopsis*, two independent lines, *rh17-1* and *rh17-2*, harboring T-DNA insertions in the eighth exon and the fifth intron, respectively, were selected for analysis. A CRISPR/Cas9 line designated *rh17-3* was also generated, leading to a frame-shift deletion in the seventh exon. Consistent with crucial roles for reproductive development, plants heterozygous for either of the three alleles showed 37% (*n*=895), 39% (*n*=1514) and 33% (*n*=233) arrested seeds or ovules in *rh17-1/RH17*, *rh17-2/RH17* and *rh17-3/RH17*, respectively, in contrast to 3% (*n*=793) observed in wild-type plants. As all lines showed seed abort at similar frequencies, only *rh17-1/RH17* and *rh17-2/RH17* were investigated in further detail.

In accordance with the high frequencies of seed abort, homozygous plants were not recovered. To describe the defect in more detail at the genetic level, we studied the segregation of the mutant alleles in the offspring of heterozygous plants by scoring sulfadiazine resistance linked to the T-DNA insertion for *rh17-1* or by genotyping of *rh17-2*. For *rh17-1/RH17*, we observed 62.0% (*n*=645) resistant seedlings and 63.5% heterozygous plants were identified by genotyping of *rh17-2/RH17* (*n*=158). These ratios of the numbers of plants carrying a mutant allele and wild-type plants differed significantly from the ratios expected for Mendelian inheritance (3:1, χ-squared=57.9 and 11.6 for *rh17-1/RH17* and *rh17-2/RH17*, respectively). Taken together with the frequencies of seed abort, the observed segregation distortion points towards an

embryo lethal defect likely combined with partially penetrant gametophytic lethality. To elucidate which parent was affected, analysis of transmission efficiency through male and female gametes was performed after reciprocal crosses of heterozygous lines to wild type (Table 1). The results indicated a slightly reduced transmission efficiency through the male, rather than the female parent. Therefore, we addressed pollen viability in *rh17-1/RH17* by Alexander staining (Peterson et al., 2010). The percentage of viable pollen was slightly reduced to 80% (*n*=531) compared with 90% (*n*=709) in wild type (Fig. S1H). Together, these data indicate that mutant alleles of *RH17* result in embryo lethality combined with a partially penetrant male gametophytic defect.

Two embryos in one seed are formed at low frequencies

As high frequencies of seed abort were observed in siliques from heterozygous plants, we used differential inference contrast (DIC) microscopy after clearing with chloral hydrate to identify developmental defects during embryo and endosperm development. In contrast to wild type, which exhibited normal seed development and formation of one embryo per seed (*n*=91), in siliques harboring maturing seeds, both lines carrying a mutant allele of *RH17* showed pleiotropic phenotypes (Fig. 1, Fig. S2). Consistent with the embryo lethal defect, in 60% (*rh17-1/RH17*) and 62% (*rh17-2/RH17*) of the seeds normal embryo and endosperm development was observed, whereas 25% of embryos were aborted typically at the globular or heart stage in both *rh17-1/RH17* (*n*=321) and *rh17-2/RH17* (*n*=227) (Fig. 1, Fig. S2). Occasionally, in seeds aborted at the globular stage of embryogenesis no endosperm was formed (Fig. 1B,D). Furthermore, in both lines, over-proliferating embryos were present in 7% of seeds (Fig. 1I, Fig. S2D,E). In addition, enlarged endosperm nuclei were
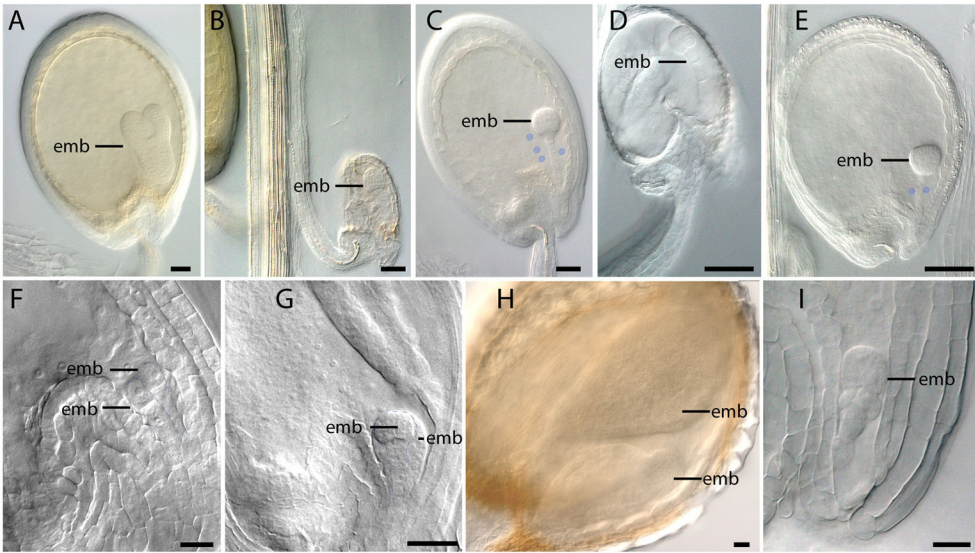

Fig. 1. Analysis of seed development in *rh17-1/RH17* and *rh17-2/RH17*. (A-I) DIC microscopy images showing typical wild-type embryo development (A), seed abortion at the early globular stage of embryo (emb) development without evidence for endosperm development in *rh17-1/RH17* (B) and *rh17-2/RH17* (D), formation of enlarged endosperm nuclei near the developing embryo (counterstained in blue) in *rh17-1/RH17* (C) and *rh17-2/RH17* (E), formation of two embryos per seed in *rh17-2/RH17* (F-H), and an overproliferated *rh17-2/RH17* embryo (I). Scale bars: 20 μm.

frequently visible close to the embryo (Fig. 1C,E). In the remaining ovules, mostly arrested or unfertilized mature gametophytes were visible, or gametophytes were lacking (Fig. S2B,C).

Interestingly, two embryos in one seed were occasionally observed (Fig. 1F-H, Fig. S3U). However, developmental defects of one embryo or differences in the developmental stage were apparent, suggesting that successful germination of both embryos is unlikely (Fig. 1G,H). To score frequencies, we analyzed siliques with seeds at early stages of embryo development (up to ~128 cell embryo proper). Two embryos and endosperm were formed in one seed at frequencies of 2.8% in *rh17-1/RH17* (n=109) and 1.5% in *rh17-2/RH17* (n=268) (Fig. 1, Fig. S3U). In summary, these observations suggest that the mutant alleles cause alterations in reproductive development and defects in the embryo and in endosperm.

The second embryo likely forms from an additional germline in the same ovule

Despite low frequencies, formation of more than one embryo per seed is exceptional in *Arabidopsis*. To gain insights into the origin of the additional embryo, we studied the formation and development of the female germline. We introgressed the p*KNU::nlsYFP* marker, which labels the MMC (Tucker et al., 2012), into *rh17-1/RH17* and *rh17-2/RH17* plants. In wild type, typically only a single enlarged

subepidermal cell, the MMC, is visible in young ovules. Nevertheless, formation of more than one enlarged cell has been reported at low frequencies of ~6% (Grossniklaus and Schneitz, 1998; Olmedo-Monfil et al., 2010; Schmidt et al., 2011). Consistent with this, in the p*KNU::nlsYFP* lines a second enlarged cell next to the MMC or female meiocyte was visible in 5.9% of scored ovules. In the vast majority of ovules only one enlarged subepidermal cell expressing the marker was observed (Fig. 2A,G, Fig. S3A,B). In contrast, in *rh17-1/RH17* carrying the marker, a second enlarged non-labeled cell was visible next to the MMC at a frequency of 23.5% (Fig. 2C,D,G, Fig. S3C,D,G), and only occasionally a second marked cell was observed (not shown). In *rh17-2/RH17*, 27.3% of ovules showed a second enlarged cell next to the MMC not expressing the marker (Fig. 2F,G, Fig. S3E,F). Based on the absence of YFP activity, we can conclude that these cells do not typically acquire MMC identity.

Whereas in wild type the rarely observed additional enlarged cells typically do not give rise to formation of gametophytic lineages (Fig. 2N,Q) (Pinto et al., 2019), the development of additional gametophytes was observed by clearings in 27.8% and 28.2% of ovules in *rh17-1/RH17* and *rh17-2/RH17*, respectively (Fig. 2O-Q, Fig. S3Q). To determine whether FMS-like cells and developing cell lineages are specified as gametophytic, we used the *ANTIKEVORKIAN* (*AKV*) reporter for cell identity (Fig. 2H-L,
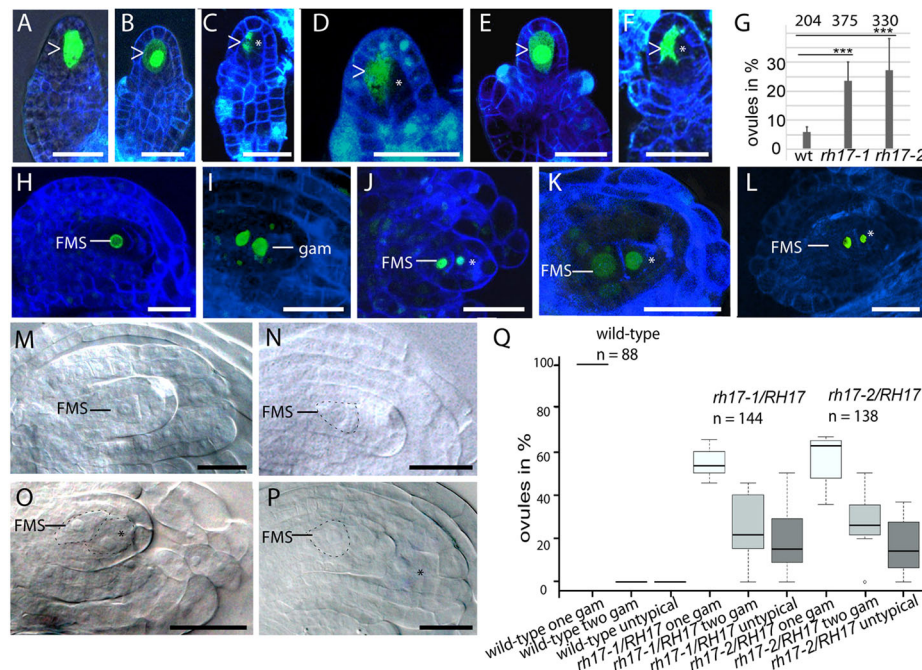

Fig. 2. Formation of two germline lineages in one ovule. In young ovule tissues of lines carrying a mutant allele of *RH17*, formation of additionally enlarged cells next to the MMC was frequently observed, which gave rise to an additional gametophytic lineage. (A-L) MMC (A-F) or gametophytic (H-L) identities are visualized with the p*KNU::nlsYFP* (Tucker et al., 2012) and p*AKV::H2B-YFP* (Rotman et al., 2005) markers, respectively, using laser-scanning confocal microscopy. SR2200 cell-wall label is shown in blue. (A-F) MMCs are indicated by arrowheads, and additionally enlarged cells are marked with an asterisk in wild type (A), *rh17-1/RH17* (B-D), and *rh17-2/RH17* (E,F). (G) Frequencies of additionally enlarged cells observed next to the MMC. Numbers above bars represent the total number of counted ovules and error bars represent s.d. Frequencies in *rh17-1/RH17* (*rh17-1*) and *rh17-2/RH17* (*rh17-2*) differ significantly from wild type (wt). ***P<0.001 (Student's t-test). Counts from at least four plants per genotype are presented. (H,I) Single wild type-like FMS (H) and two-nucleate gametophyte (gam) (I) in *rh17-1/RH17*. (J-L) Two FMS-like cells labeled as gametophytic in *rh17-1/RH17* (J,K) and *rh17-2/RH17* (L). Asterisks mark additional FMS-like cells. (M-P) DIC microscopy images showing a wild type-like ovule with a single FMS in *rh17-1/RH17* (M), an ovule with a single FMS in wild type (N), and an additional FMS-like cell adjacent to the FMS in *rh17-1/RH17* (marked with an asterisk in O) and at an atypical position in the ovule in *rh17-1/RH17* (marked with an asterisk in P). (N-P) The FMS (N,P) or the FMS and an additional FMS-like cell (O) are encircled by dashed lines. (Q) Box and whiskers plot showing frequencies of ovules with a single FMS/gametophyte (one gam), additional gametophytic lineages (two gam), or atypically positioned gametophytic nuclei (untypical). The black line in the box designates the median, the ends of the boxes show the upper and lower quartiles, and whiskers designate highest and lowest values excluding outliers. Counts from at least four plants per genotype are presented. Scale bars: 20 μm.

Fig. S3H-P,R-T,V), which is active in female gametophytic nuclei from the FMS stage to cellularization (Pillot et al., 2010; Schmidt et al., 2011). Consistent with our expectations, gametophytic identity could be confirmed based on the activity of the *AKV* reporter. In addition, atypical positioning of gametophytic nuclei in the ovule likely results from more than one gametophyte per ovule (Fig. S3M-P,R-T,V). In contrast to the p*AKV::H2B-YFP* marker line serving as control (Fig. S3J-L,V), the occurrence of ectopically formed gametophytes was also occasionally detected in *rh17-1/RH17* and *rh17-2/RH17* expressing the reporter construct (Fig. S3M-O,R).

Interestingly, different sizes of gametophytic nuclei were sometimes presented in the same ovule, which might indicate different ploidies of the nuclei (Fig. 2J-L). To determine whether cells other than the MMC undergo meiosis, we used the KINGBIRD marker line, which allows visualization of the activity of the core meiotic protein REC8 (Prusicki et al., 2019). However, only the MMC was labeled as meiotic in young ovules of *rh17-1/RH17* (*n*=43) (Fig. S4). Taken together, in the lines carrying mutant *RH17* features resembling apospory were displayed, where an additionally enlarged sporophytic cell adjacent to the MMC potentially initiates gametogenesis without undergoing meiosis.

However, in agreement with the fact that two embryos were observed only infrequently, the additionally formed gametophytes rarely reached maturity (Figs S5E and S6I). Most of the additionally formed gametophytes appeared to arrest at early stages of gametogenesis (Fig. S6G,H). Furthermore, no evidence for mis-specification of gametophytic cells was given in mature gametophytes of *rh17-1/RH17* carrying a multicolor fluorescent marker line labeling each cell of the mature gametophyte with a different fluorescent protein at 2-3 DAE (Fig. S5). This suggests that the second embryo likely derived from an egg cell of a second gametophyte that formed in the same ovule.

Features of autonomous seed development initiate in the absence of fertilization

The question remains regarding how two embryos and functional endosperm can form in one seed, as typically during double fertilization only one sperm cell each is delivered to the egg and the central cell. Therefore, we tested for the possibility of autonomous embryo or endosperm development. To this aim, we emasculated floral buds and subjected the ovules to clearing at 5 DAE (Fig. S6). A tendency was identified for an enlargement of ovules and the formation of additional nuclei in lines carrying a mutant *rh17* allele. To gain more insight into developmental changes over time, we further analyzed ovules at 6-7 DAE. Unlike in wild type (*n*=284), we observed an enlargement of ovules and features of autonomous seed coat formation at frequencies of 11.4% and 12.1% in *rh17-1/RH17* (*n*=667) and *rh17-2/RH17* (*n*=331), respectively (Fig. 3). In addition, evidence of autonomous endosperm formation, mostly with low numbers of nuclei, was observed in 7.5% and 9.4% of ovules from *rh17-1/RH17* and *rh17-2/RH17*, respectively (Fig. 3B-D,F). Nevertheless, endosperm identity was not unambiguously confirmed and an origin of nuclei by proliferation of gametophytic nuclei cannot be ruled out. To confirm parthenocarpy, vanillin staining forming a red color upon reaction with proanthocyanidins in the developing seed coat was applied at 7 DAE (Xuan et al., 2014). The staining supported the hypothesis of autonomous seed coat development (Fig. 4).

Unlike these features of autonomous seed development, we did not find evidence for autonomous embryo formation. To test whether offspring were derived by fertilization, we used *rh17-1/RH17* (Ecotype Col-0) as a mother and the AKV- or multicolor fluorescent marker lines (Ecotype Landsberg *erecta*, L*er*) as father. We used established mapping primers to identify L*er* alleles in 105 seedlings (Zhang et al., 2007). In all plants tested, the presence of L*er* genomic information was confirmed (Fig. S7). This suggests that offspring is usually formed by fertilization of the egg cell.

Transcriptome analysis suggests deregulation of genes related to ribosome biosynthesis, stress response, hormonal pathways and seed coat development

Autonomous endosperm and seed coat development typically involve a derepression or deregulation of genes and pathways repressing such development. To identify genomic pathways involving the activity of *RH17*, we used RNA-Seq for
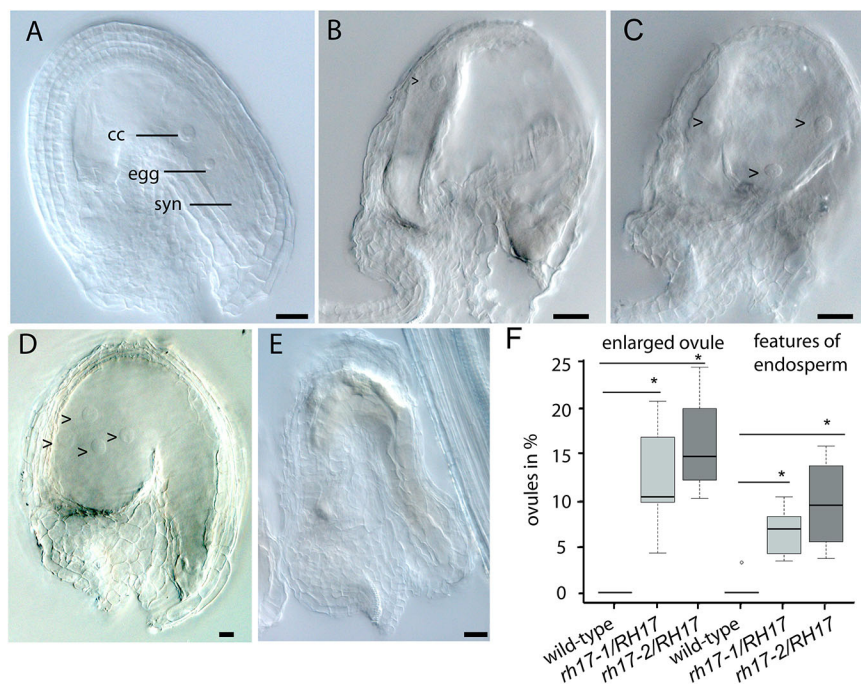

Fig. 3. Features of autonomous endosperm and seed coat development. (A-D) Wild type-like ovule (A), and formation of endosperm-like nuclei (indicated by arrowheads) in *rh17-1/RH17* (A-C) and *rh17-2/RH17* at 6 DAE (D). Embryos are not formed, suggesting autonomous development. For B,C, two optical sections of the same ovule are presented. (E) Features of parthenocarpy in *rh17-1/RH17* at 6 DAE. cc, central cell; egg, egg cell; syn, synergid cells. Scale bars: 20 μm. (F) Box and whiskers plot presenting the percentage of enlarged ovules or two or more nuclei likely representing early stages of endosperm formation in wild type (absent, *n*=284), *rh17-1/RH17* (*n*=667) or *rh17-2/RH17* (*n*=331) at 6-7 DAE. The black line in the box designates the median, the ends of the boxes show the upper and lower quartiles, and whiskers designate highest and lowest values excluding outliers. Counts from at least four plants per genotype are presented. Significant differences compared with the wild type were confirmed by Student's *t*-test (**P*<0.05).
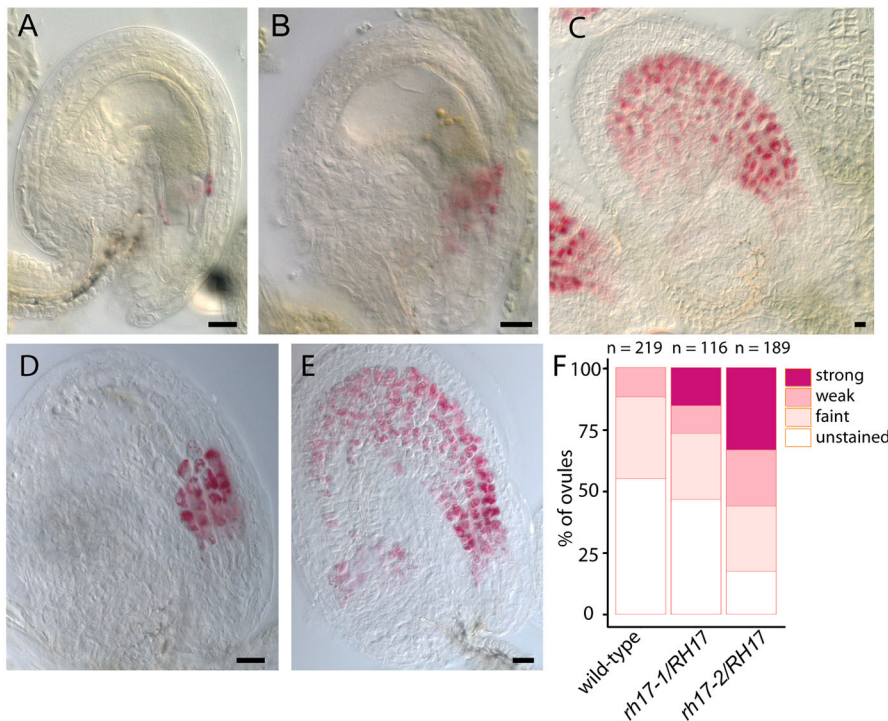
Fig. 4. Autonomous seed coat development. Vanillin stain resulting in a red complex with proanthocyanidins forming upon seed coat development identified at 7 DAE. (A,B) Ovules of wild type showing no staining or very faint staining (A) or weak staining (B). (C) Strong staining in *rh17-1/RH17*. (D,E) Weak (D) and strong (E) staining in *rh17-2/RH17*. Scale bars: 20 µm. (F) Percentages of ovules from wild type, *rh17-1/RH17* or *rh17-2/RH17* showing no staining, or faint, weak or strong staining. The distribution of staining intensities observed in *rh17-1/RH17* and *rh17-2/RH17* differed significantly from wild type (Fisher's exact test; *P*<0.001). Counts from at least three plants per genotype are presented.

transcriptional profiling of ovules at 3 DAE. In the wild type, gametophytes are fully mature at this stage, whereas we expect the developmental programs enabling autonomous development to be activated in the lines carrying a mutant allele of *RH17*. Illumina Next Seq500 was used to sequence three and two biological replicates of RNA isolated from ovules of wild type or *rh17-1/ RH17*, respectively. This resulted in between 41,637,502 and 60,884,568 paired mapped reads per sample after quality control and trimming (Table S1). We found that 19,726 genes were expressed in all samples of *rh17-1/RH17* and the wild type, whereas only 374 and 396 genes were active either in both samples of *rh17-1/RH17* or all three replicates from the wild type at ≥10 TMM normalized read counts, respectively (Fig. S8A). Compared with the wild type, 1558 genes were identified as differentially regulated in ovules of *rh17-1/RH17* (FDR ≤0.05 after Benjamini–Hochberg adjustment) (Robinson et al., 2009) (Tables S2 and S3, Fig. S8B). As only a heterozygous line could be used for this analysis, the tissues of *rh17-1/RH17* contained a mixture of heterozygous maternal sporophytic tissues of the ovule harboring on average about 50% gametophytes carrying the *rh17-1* allele and 50% wild-type gametophytes. Consequently, the fold changes (FC) observed for differential expression will be reduced (Table S3). For example, a 0.6 log FC was observed for *RH17*. Interestingly, the DEGs identified with the highest FC included (long) non-coding RNAs (Table S3). For the long non-coding RNA AT1G07887, we independently validated this great change in abundance by real-time PCR (Fig. S9).

To categorize the gene regulatory programs and to identify biological processes that are over-represented in the set of genes, we analyzed Gene Ontology (GO) enrichment. Biological processes that were upregulated (*P*<0.01) pointed towards the relevance of stress responses including redox-related processes and salt stress, hormonal pathways related to auxin, gibberellin and jasmonic acid, and ribosome-related processes (i.e. GO:0034976 'response to endoplasmic reticulum stress' and GO:0034620 'cellular response to unfolded protein') (Table S4). Interestingly, the DEGs

representing the biological process of 'response to endoplasmic reticulum stress' included the luminal binding proteins BIP1 and BIP2, which are relevant for fusion of polar nuclei prior to endosperm proliferation (Table S5) (Maruyama et al., 2020). The category related to redox regulation comprised a number of cytochrome P450 genes, including *CYP78A5* (also known as *KLUH*, *KLU*), previously reported to have roles in regulation of reproduction during germline specification and to control seed size and seed coat development (Adamski et al., 2009; Zhao et al., 2018). Apart from *KLU*, *AGAMOUS-LIKE 11* (*AGL11*; also known as *SEEDSTICK*, *STK*), *CYTOKININ OXIDASE/ DEHYDROGENASE 1*, *UBIQUITIN-SPECIFIC PROTEASE 15*, *ABA DEFICIENT 2*, *ABSCISIC ACID-INSENSITIVE 5* and *DA* (*LARGE IN CHINESE*) *2* were among the DEGs with reported roles in control of seed size (Orozco-Arroyo et al., 2015). Furthermore, *YUCCA6*, which is an important player in auxin synthesis (Robert et al., 2015), was identified as one of the DEGs more highly expressed in *rh17-1/RH17* ovules compared with the wild type. The category of auxin-responsive DEGs comprised 52 genes, including *AUXIN RESPONSE FACTOR 5* (*ARF5*), *ARF18*, a number of *SMALL AUXIN UPREGULATED RNA* (*SAUR*) genes, different *INDOLE-3-ACETIC ACID INDUCIBLE* (*IAA*) genes, in addition to *PIN-FORMED 7* (*PIN7*), *PIN3* and *GH3.6* (Table S5). Importantly, transcriptional regulation was also identified as an upregulated term (GO:0006355, 'regulation of transcription, DNA templated') (Table S4). This category comprised 152 DEGs, including a number of AGL MADS box genes, such as *SEPELATA2* (*SEP2*), *SEP3*, *DIANA*, *STK*, *AGL20*, *AGL99*, and others, e.g. *BASIC HELIX-LOOP-HELIX PROTEIN 100* (*BHLH100*) (Table S5). In addition to metabolic processes, developmental processes were also affected, including GO:0080155 'regulation of double fertilization forming a zygote and endosperm'. In good agreement with our observations, the biological process of 'seed coat development' (GO:0010214) was enriched (Fig. 5, Tables S4 and S5). Interestingly, all genes in this category were significantly more highly expressed in our lines carrying a mutant *rh17-1* allele
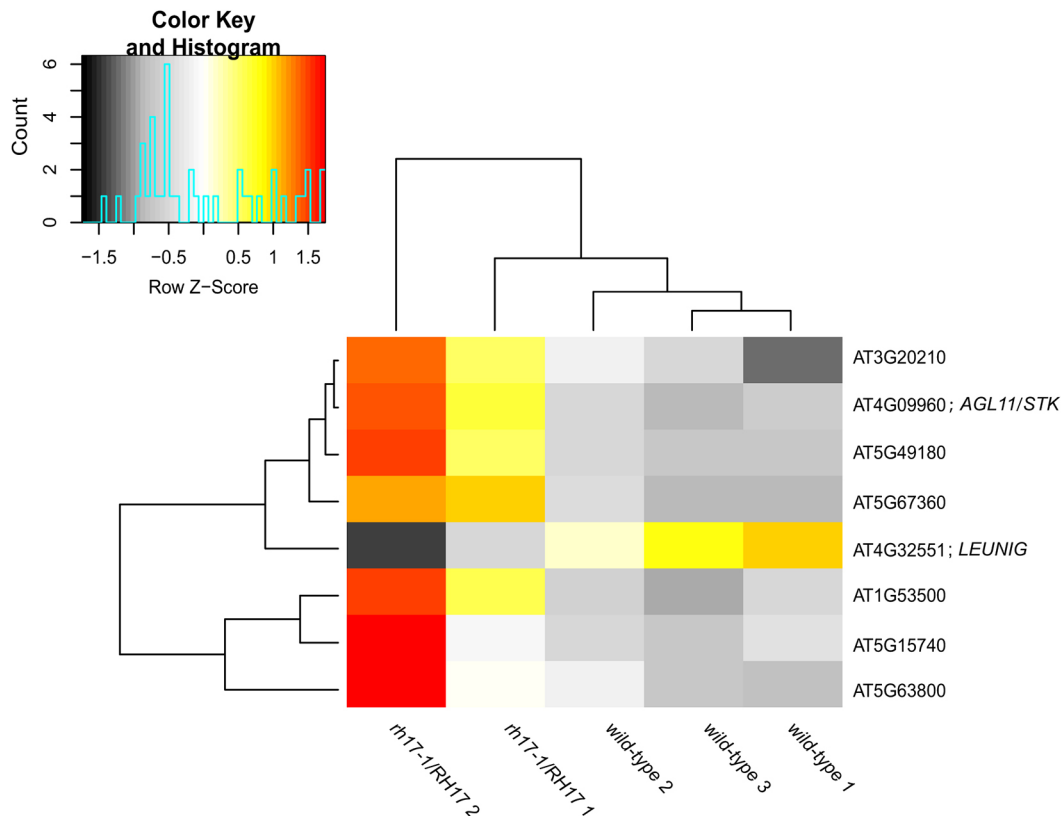
6

Fig. 5. Visualization of expression levels of DEGs involved in seed coat formation. Heatmap of log2-transformed mean expression values. Hierarchical clustering of genes and samples was based on Euclidean distance and agglomerative hierarchical clustering. Red denotes high expression and black low expression.

compared with the wild-type ovules, with the exception of *LEUNIG*, which is a regulator of seed coat mucilage extrusion (Bui et al., 2011). Importantly, *STK*, which is upregulated in our lines carrying a mutant allele, has previously been reported to be a master regulator of seed coat development (Mizzotti et al., 2014). Furthermore, epigenetic regulation, in particular 'histone lysine demethylation', was differentially regulated (Tables S4 and S5). Taken together, the data indicate differential regulation of a number of genes and pathways, including, importantly, known regulators of reproductive development.

DISCUSSION

In natural apomicts, several alterations compared with sexual reproduction are required, including the formation of an unreduced gametophytic lineage, and the coordinated development of the parthenogenetic embryo and of endosperm. Despite several decades of research, the longstanding dream of engineering apomixis into crops has not been accomplished to date. Nevertheless, as a proof of concept, clonal offspring has been obtained in sexual plants by combinations of mutations in three meiotic genes and systems for haploid induction (Marimuthu et al., 2011; Schmidt, 2020). Whereas haploid induction requires egg cell fertilization prior to elimination of the paternal genome, even parthenogenesis can be induced in rice by expression of the transcription factor *BABY BOOM 1* in the egg cell (Khanday et al., 2019). The applicability of these genes and systems is thus far limited, as typically clonal offspring is only obtained at low frequencies (Scheben and Hojsgaard, 2020). Furthermore, it would be a great advancement if less complex breeding systems could be established with the requirement to modify fewer genes. In partial contradiction to the

longstanding hypothesis of apomixis being derived from deregulation of the underlying gene regulatory program of sexual reproduction (Carman, 1997), it is typically genetically linked to one or a few loci (Barcaccia and Albertini, 2013). This has previously stimulated the idea of a master regulator that might be in control of a complex regulatory program (Eckardt, 2003). Here, we demonstrate that mutant alleles of *RH17* lead to alterations in sexual development resembling different features of apomixis. Although a straightforward application is not foreseeable owing to the embryo lethality observed, these findings suggest that it might be possible to induce more than one element of apomixis by manipulation of one or a few genes only.

Interestingly, low frequencies of formation of two mature gametophytes in one ovule and of polyembryony have previously been observed in natural apomicts of the genus *Boechera* (Carman et al., 2019). This is similar to our observations in *Arabidopsis* lines carrying a mutant allele of *RH17*. Here, we cannot exclude the possibility that two embryos and functional endosperm derive from fertilization processes involving the attraction of more than one pollen tube, which occurs at low frequencies in *Arabidopsis* (Maruyama et al., 2013). Nevertheless, we provide evidence for parthenocarpy and potentially also autonomous endosperm development, suggesting an alternative explanation. Although viable offspring typically derived from fertilization of the egg cell, the embryo lethal defect suggests that gene regulatory programs governing embryogenesis might be imbalanced.

In contrast to the tight control of seed formation, greater developmental flexibility is observed upon germline specification. Increasing evidence suggests that complex gene regulatory systems are required to mediate the important developmental transition from

sporophytic to gametophytic fate, the repression of multiple reproductive lineages per ovule, and the commitment of the MMC to meiosis (Lora et al., 2019). Accordingly, several types of mutants in which surplus germlines develop have been described, mainly differing in the fate of the MMC or the sporophytic cells acquiring germline identity (Pinto et al., 2019; Schmidt et al., 2015; Su et al., 2020; Zhao et al., 2018, 2017). Unlike in several other mutants, but similar to lines carrying a mutant allele of *RH17*, in *stk* mutants the p*KNU::nlsYFP* marker for MMC identity is typically not active in additional enlarged subepidermal cells (Mendes et al., 2020). Although *STK* was deregulated in ovules at 3 DAE, it remains to be determined whether RH17 also affects the expression of this gene at early stages of reproduction. Furthermore, ectopic MMCs in mutant lines of *SET DOMAIN GROUP 2*, an epigenetic regulator of H3K4 methylation, are not consistently labeled with the marker *KNU* (She, 2014; Yao et al., 2013). The control of histone modifications, specifically the eviction of repressive H3K27me3 marks established by PRC2, is crucial for activation of *KNU* (Sun et al., 2014). Therefore, it is possible that the epigenetic setup prevents activation of *KNU* in ectopic cells adjacent to the MMC. Together with the low, or lack of, expression of the *KNU* homolog in *Boechera* nucellus tissues (Zühl et al., 2019), this could be an indication that KNU activity is not generally required upon germline specification. Interestingly, KNU is involved in repression of the gene encoding the homeodomain protein WUSCHEL (WUS), which is an important regulator of stem cell fate (Sun et al., 2014). As repression of *WUS* is crucial for entry into meiosis (Zhao et al., 2017), in our lines the additional enlarged cells potentially do not express *KNU* as they likely do not become committed to meiosis, in agreement with the lack of REC8 activity. Therefore, the control of *KNU* itself might depend on meiotic fate of the MMC rather than on germline identity.

An important question remaining is the molecular mechanism involving RH17 that leads to the restriction of germline fate to one cell lineage per ovule. As *RH17* is expressed in the MMC and in surrounding nucellus tissues, both cell-autonomous and non-cell-autonomous mechanisms might be involved. Interestingly, similar apospory-like phenotypes can be obtained by modifications of other genes, including *MEM* (Schmidt et al., 2015, 2011). Therefore, redundancy is unlikely, as the underlying genetics of the developmental defects differ, with mutations in *MEM* leading to a female gametophytic defect and mutations in *RH17* causing embryo lethality combined with a slightly reduced transmission efficiency through the male parent. The cause of this remains to be elucidated, but it is possible that RH17 acts in certain RNPs that are important during pollen development and pollen tube growth (Honys et al., 2009).

Evidence for the involvement of RH17 in ribosome biogenesis has previously been described for homologs in yeast and rice (Liu and Imai, 2018; Xu et al., 2015). This is in agreement with the deregulation of ribosome-associated processes identified in our transcriptional analysis. Biogenesis and function of ribosomes is highly dynamic and an important level of translational regulation (Dalla Venezia et al., 2019). Previously, for an *Arabidopsis* line conferring overexpression of *RH17*, implications for response to salt stress have been demonstrated as well as a decreased accumulation of reactive oxygen species (Nguyen et al., 2018). In contrast, overexpression or knockdown of the rice homolog did not affect sensitivity to different biotic or abiotic stress treatments (Xu et al., 2015). The over-representation of biological processes related to endoplasmic reticulum stress and protein folding, in combination with responses to salt stress and redox regulation, suggests that

AtRH17 might function in the regulation of stress response via association with ribosomes. This is consistent with previous reports that mutations in genes involved in ribosomal pathways lead to increased sensitivity to salt stress (Palm et al., 2019). Alternatively, deregulation of processes involved in the stress response might be a consequence of a proteotoxic effect resulting from imbalanced ribosome biosynthesis, as recently demonstrated for *Saccharomyces cerevisiae* (Albert et al., 2019). Given this, the higher tolerance of overexpression lines to salt stress might reflect a stabilization of ribosomal processes. Moreover, upregulation of processes related to hormonal, epigenetic regulatory, and developmental pathways could serve as an indication that RH17 integrates the control of developmental processes in response to environmental conditions. In agreement with the differential activity of genes involved in auxin synthesis, transport and signaling, auxin has been shown to play important roles in ribosome biosynthesis (Rosado et al., 2010). In turn, ribosomes are involved in regulation of auxin signaling, and, for example, translational control of *ARF5*, which is an important regulator of embryo development, is mediated by ribosomes (Merchante et al., 2017; Rosado et al., 2012). Interestingly, *ARF5* was one of the DEGs identified in our study. Consistent with the importance of auxin signaling for embryo development and patterning control (Möller and Weijers, 2009), the observed over-proliferation of embryos might result at least in part from the deregulation of auxin signaling. This suggests that RH17 acts in ribosomal pathways potentially both controlling and being under the control of auxin signaling.

The upregulation of *YUCCA6* indicates that auxin synthesis might be enhanced in ovules carrying a mutant *rh17* allele. Importantly, auxin can induce autonomous seed coat and endosperm development (Figueiredo et al., 2016; Figueiredo and Köhler, 2018). This pathway also involves the activity of different AGL MADS box transcription factors, which are generally broadly active and involved in the regulation of gametophyte and seed development (Bemer et al., 2010). In particular, AGL62 mediates the transport of auxin from endosperm to seed coat to induce development (Figueiredo et al., 2016). Furthermore, *AGL36* shows increased expression in response to elevated auxin levels (Batista et al., 2019; Shirzadi et al., 2011). Although neither of these were identified as DEGs at 3 DAE, we cannot rule out the possibility that differential regulation might occur at later stages of autonomous seed development. In contrast, *DIANA*, a gene crucial for central cell development and specification, mutants of which fail to give rise to endosperm formation (Steffen et al., 2008), was identified as DEG. Interestingly, defective or failed endosperm formation was observed in a number of seeds. However, mutant alleles of *RH17* also induce features of autonomous endosperm development. Mostly low numbers of nuclei were observed, indicating that endosperm nuclei likely only undergo first divisions, but in cases of two nuclei the possibility of persistent unfused polar nuclei of the central cell cannot be unambiguously excluded. In wild type, autonomous endosperm development and parthenocarpy are typically repressed by PRC2 activity. Interestingly, long non-coding RNAs are involved in recruitment of PRC2 complexes to target sites (Brockdorff, 2013). Whether RH17 plays a role in this pathway remains to be elucidated by future studies.

Increasing evidence suggests that RNA helicases may play a role in gene regulation by association with mechanisms involving non-coding RNAs (Nair et al., 2020; Schmidt, 2020). Our transcriptional analysis identified (long) non-coding RNAs as differentially expressed with high levels of fold changes, for example AT1G07887, which potentially modulates the activity of

HOMOLOG OF HUMAN HEI 10, a gene involved in meiotic crossover formation (De Muyt et al., 2014; Ziolkowski et al., 2017). Consistent with previous reports of RH17 being involved in the formation of R-loops, which represent DNA-RNA hybrids and associated single-stranded DNA, functional roles of RH17 during meiosis in the control of genome integrity are likely (Castellano-Pozo et al., 2012; Santos-Pereira and Aguilera, 2015; Xu et al., 2020).

In our lines carrying mutant alleles of *RH17*, pleiotropic phenotypes were observed, consistent with the deregulation of various genes. It remains to be uncovered which of the DEGs are direct targets and which are indirectly affected in their expression. Interestingly, the mechanism of action of RH17 likely resides in ribosomal-associated pathways, underpinning the notion that specialized ribosomes might play a crucial role in the modulation of gene activity. In conclusion, we uncovered RH17 as a player in the control of plant reproductive development. Strikingly, several alterations of sexual development were observed, including features resembling apomixis. Our findings suggest that hormonal pathways, ribosomal pathways and regulation via non-coding RNAs are involved, providing an excellent basis for future studies investigating the specific molecular mechanisms and machineries underlying underlying the developmental alterations caused by mutant alleles of *RH17*.

MATERIALS AND METHODS
Plant material
Arabidopsis thaliana (L.) Heynh. Ecotype Col-0 was used as wild type. T-DNA insertion lines were obtained from the Eurasian *Arabidopsis* Stock Centre (NASC, http://arabidopsis.info/) and GABI-Kat (https://www.gabi-kat.de/). The multicolor fluorescent marker line [in Landsberg *erecta* (L*er*) genomic background] to label the cell types of the mature female gametophyte has been described previously (Lawit et al., 2013). Seeds of the p*KNU::nlsYFP* (Tucker et al., 2012), the p*AKV::H2B-YFP* (in L*er* genomic background) (Rotman et al., 2005), and the KINGBIRD (Prusicki et al., 2019) marker lines were kindly provided by Matthew Tucker (University of Adelaide, Australia), Weicai Yang (Beijing University, Beijing, China) and Arp Schnittger (University of Hamburg, Germany), respectively. The lines were introgressed into *rh17-1/RH17* and *rh17-2/RH17*, and F1 or F2 offspring of the crosses were analyzed. Seeds were stratified for at least 1 day in darkness before surface sterilization as described previously (Wuest et al., 2010). Seedlings were germinated and grown on Murashige Skoog (MS) plates for about 2 weeks before transfer to soil (ED73, Universalerde, Germany). Subsequently, plants were grown in a growth chamber at 16 h light/8 h darkness at 21°C and 18°C, respectively. Plants were treated with nematodes against fungus gnats.

Generation and characterization of mutant plant lines
Two independent T-DNA insertion lines disrupting the eighth exon and the fifth intron of the gene *AT2G40700* encoding for RH17 (*rh17-1* and *rh17-2*, which are GABI_814E05 and SALK_076414, respectively) were obtained from GABI-Kat and NASC. Lines *rh17-1* and *rh17-2* were genotyped with primers 5′-CTCCCTTGTGAGCTGCATATC-3′, 5′-ATGGAATACCAT-CACAGCTGG-3′ and the left border (LB) primer 5′-GGGCTACACT-GAATTGGTAGCTC-3′, or with primers 5′-CGATCTCTACGAGA-CACTGGC-3′, 5′-AAAAGCAAAGATTTAGAAGATTTAAATC-3′ and the LB primer 5′-ATTTTGCCGATTTCGGAAC-3′, respectively. Positions of T-DNA LBs were confirmed by sequencing to be inserted after base 1769 on genomic DNA counted from the A of the start codon for *rh17-1* and after base 938 for *rh17-2*. Linkage of sulfadiazine resistance to the locus of the *rh17-1* insertion was verified by genotyping. For investigation of segregation distortion, offspring of heterozygous plants carrying the *rh17-1* or *rh17-2* mutant alleles were analyzed either by counting the ratio of plants sensitive or resistant to sulfadiazine or by genotyping, respectively. Resistance was tested on MS medium supplied with 7.5 mg/l sulfadiazine. Analysis of transmission efficiency was performed by

reciprocal crosses of *rh17-1/RH17* and *rh17-2/RH17* to wild type and subsequent analysis of the presence of the mutant allele by scoring sulfadiazine resistance or by genotyping, respectively.

Generation of the CRISPR/Cas9 line was carried out as previously described (Kiefer et al., 2020), except that small guide RNAs 5′-ATT-GTGCAGTGCCATGTGGTGCA-3′ and 5′-AAACTGCACCACATGG-CACTGCA-3′ were used and genotyping was performed with primers 5′-ACCATCACAGCTGGTACAGAGA-3′ and 5′-CAGGAACTTCTGGC-TTGAGATT-3′ and the restriction enzyme ApaLI (New England Biolabs). To generate the line *rh17-3/RH17*, a heterozygous mother plant was crossed to wild type. The offspring resulting from this cross was germinated on MS plates with hygromycin and sensitive plants were rescued. Genomic DNA was isolated from sensitive plants and tested for the absence of the CRISPR/Cas9 construct with primers 5′-GATTTCATGCTCACACATGCTC-3′ and 5′-GAAGAGCTGGTTGTACGTCTG-3′. A frameshift deletion of GT in the target region after base 1430 (counted on genomic DNA from the A of the start codon) was confirmed by amplification of the region with the primers used for genotyping, cloning of the PCR construct into pJET1.2/blunt (Thermo Fisher Scientific) and sequencing of five clones using the T7 primer.

Test for clonal offspring by use of mapping primers
To test for potential formation of clonal offspring, *rh17-1/RH17* plants were emasculated for 2-3 days prior to pollination with either the p*AKV::H2B-YFP* marker line or the multicolor fluorescent marker line both representing L*er* ecotype. Sulfadiazine-resistant F1 offspring was tested for the presence of L*er* genomic DNA by using primers for map-based cloning with Col-0 and L*er* ecotypes with the primer combination T2E12F and T2E12R (Zhang et al., 2007). PCR products were analyzed on 1% agarose gels stained with GelRed (Biotium).

Subcellular localization in *Nicotiana benthamiana*
The AtUBIQUITIN10::RH17-mVENUS construct for transient expression in *Nicotiana benthamiana* was assembled using the GreenGate cloning system (Lampropoulos et al., 2013). To generate the pGGC-*RH17* module, the coding sequence of *Arabidopsis RH17* was amplified with Phusion (New England Biolabs) using primers 5′-AACAGGTCTCAGGCTCAA-CAATGATGAAGAGAGCCCAACAATC-3′ and 5′-AACAGGTCTCT-CTGAAGTTTTTTGTGTACTTCTATTGCC-3′. Sanger sequencing to confirm the sequence was performed at Eurofins Genomics (Ebersberg, Germany). pGGD-mVenus was kindly provided by Rainer Waadt [Centre for Organismal Studies (COS), Heidelberg University, Germany]. pGGA006, pGGB003, pGGZ003, pGGE-tHSP18.2 M and pGGF-HygR were described previously (Lampropoulos et al., 2013; Waadt et al., 2017). Assembly of GreenGate modules pGGA006, pGGB003, pGGC-*RH17*, pGGD-mVENUS, pGGE-tHSP18.2 M and pGGF-HygR into pGGZ003 was performed as previously described (Lampropoulos et al., 2013). The pUBI10::H2B:RFP::term construct (Lucas et al., 2013) used as marker for localization to the nucleus was kindly provided by Alexis Maizel (COS, Heidelberg, Germany). The expression constructs were independently transformed into the *Agrobacterium tumefaciens* ASE strain harboring the pSOUP plasmid, and bacterial cultures were mixed directly before they were used for leaf infiltration of *N. benthamiana* as described (Chen et al., 2013).

Morphological characterization by clearing and microscopy
Quantification of aborted ovule or seed development was performed after opening siliques with dissecting needles. To characterize and quantify germline and seed development, inflorescences, buds or siliques were fixed in an ice-cold mixture of 75% ethanol and 25% acetic acid, infiltrated by vacuum twice for 15 min before incubation in fixative on ice overnight followed by replacing the fixative with 70% (v/v) ethanol. Clearing was accomplished in chloral hydrate/glycerol/water (8:1:2; w/v/v) or with Hoyer's solution (Anderson, 1954). Ovules and seeds were microdissected with dissecting needles prior to microscopy. They were mounted in 80% (w/v) glycerol for epifluorescence microscopy or in 5% (w/v) glycerol with 0.1% (v/v) of the cell wall dye Renaissance 2200 (SR2200) for laser-scanning confocal microscopy (Musielak et al., 2015). Laser-scanning

confocal microscopy was performed with a Leica TCS SP8 microscope using a 63× oil immersion objective and Leica LAS X software. Images were acquired sequentially. Excitations/emissions were set to 405/410-519 nm for SR2200, and 514/519-659 nm for YFP. To score frequencies of ovules showing activity of the p*KNU::nlsYFP* and p*AKV::H2B-YFP* marker lines, laser-scanning confocal microscopy or epifluorescence microscopy were used. To score wild-type ovules expressing the multifluorescent marker line, wild-type segregants of *rh17-2/RH17* carrying the construct were used. Differential inference contrast (DIC) and epifluorescence microscopy were performed using a Zeiss Axio Imager M1 to capture images. For Alexander staining, images were taken with a Zeiss Axioskope HBO50 connected to an Axiocam MrC5 camera. Images were processed in ImageJ2.1 or processed and cropped in Adobe Photoshop CS2 Version 9.0 (Adobe Systems).

RNA-Seq on microdissected ovules
Two and three biological replicates of ovules harboring mature gametophytes 3 DAE were isolated with dissection needles from *rh17-1/RH17* and wild type, respectively. Per sample, approximately 150-200 ovules were collected and immediately frozen in liquid nitrogen. Ovule tissues were disrupted using glass beads and a mixer mill prior to isolation of total RNA using the PicoPure RNA isolation Kit (Arcturus) following the manufacturer's instructions including DNaseI digest. RNA integrity was confirmed using RNA Pico Chips on an Agilent 2100 Bioanalyzer. Libraries for RNA-Seq were prepared with the NEBNext Ultra II Directional RNA Library Prep Kit for Illumina (New England Biolabs) using NEBNext Multiplex Oligos for Illumina (Index Primers Set 1 and Index Primers Set 2) for sample indexing. Sequencing was performed on an Illumina NextSeq500 instrument by the Deep Sequencing Core Facility of Heidelberg University using the 75 bp paired end protocol.

Data analysis
The quality of raw reads was controlled with fastQC version 0.11.4 (https://www.bioinformatics.babraham.ac.uk/projects/fastqc/). Cutadapt 1.14 was used for trimming adapters and low-quality bases with the parameters set to hard trimming of the final base, and a 3′ trimming with a cutoff of phred score threshold 20 (Martin, 2011). Reads shorter 30 bp were filtered out. The TAIR10 *A. thaliana* genome sequence and Araport11 genome annotations were downloaded from Araport (araport.org) and used for mapping with Star version 2.5.3a_modified (Dobin et al., 2013). The number of fragments of correctly paired reads, of which at least 70% of read length mapped to an exon, was determined using featureCounts in Rsubread package (version 1.20.6), based on usage described by Schmid (2017). Subsequent analysis of DEGs was carried out using the Bioconductor library EdgeR implemented in R for filtering of genes with low expression and estimations of dispersions using pairwise comparisons of wild-type and *rh17-1/RH17* samples (Robinson et al., 2009). Genes with FDR <0.05 after Benjamini–Hochberg adjustment were considered to be significantly differentially expressed. The Bioconductor package topGO (http://www.bioconductor.org/packages/release/bioc/manuals/topGO/man/topGO.pdf) was used to test for the enrichment of molecular functions and biological processes. To this aim, the ATH_GO_GOSLIM annotations were downloaded from TAIR (arabidopsis.org) and used for custom gene2GO annotations in topGO. To test for overrepresented GO terms, Fisher's exact test was used combined with the function 'weight'.

Heatmap visualization of expression values
For analysis of expression, 24 DEAD-box RNA helicases were selected with homologies to yeast and human ribosomal binding factors (Liu and Imai, 2018). To analyze expression in 74 different *Arabidopsis* cell and tissue types, data were used as described previously (Kotliński et al., 2017). *RH17* was designated as present (P) when present in at least two out of three or three out of four replicates, and otherwise referred to as absent (A). Analysis of presence or absence in each sample was described previously (Schmidt et al., 2011). The heatmap in Fig. S1A was based on log2-transformed mean expression values as described (Schmidt et al., 2011). To generate the heatmap in Fig. S1B, normalized log2-transformed read counts from

RNA-Seq on *Arabidopsis* and *Boechera gunnisoniana* cell and tissue types were used as described previously (Schmidt et al., 2014). For all heatmaps presented, the heatmap.2 function implemented in the Bioconductor package gplots (https://cran.r-project.org/web/packages/gplots/gplots.pdf) was used to generate the heatmap using agglomerative clustering (complete linkage) and Euclidean distance. The Venn diagram was created with the online tool Venny 2.1 (https://bioinfogp.cnb.csic.es/tools/venny/).

Statistical analysis and visualization
Bar graphs and box and whiskers plots were created in R (www.r-project.org) with the package ggplots2 (Wickham, 2016) or with the function boxplot() using default settings. Two-sided Fisher's exact test for count data was performed in R using the fisher.test() function. Two-sided Student's *t*-test was performed in R using the function t.test().

Real-time quantitative PCR
For independent validation, three independent replicates of ovules from wild-type plants and *rh17-1/RH17* were collected from buds 3 DAE. Ovule collection and RNA isolation was carried out as described above for RNA-Seq. For cDNA synthesis, 500 μg of total RNA were used with oligo (dT) primers 12-18 (Thermo Fisher Scientific) and the Superscript IV Reverse Transcriptase Kit (Thermo Fisher Scientific) following the manufacturer's instructions. qPCR was subsequently performed on cDNA (diluted 1:30) using Luna Universal qPCR Master Mix (New England Biolabs) following the manufacturer's instructions on a Rotor Gene 6000 cycler (Corbett Life Science). Three technical replicates each were included in the analysis. Primer combinations 5′-CAAGTCATTCGACCAAAACA-3′ and 5′-GTG-AATTTCGGTTGGGTAGC-3′, and 5′-ACTCTTGAGGTGGAGAGTT-CTG-3′ and 5′-GAAGATCAGCCTCTGCTGGTC-3′, were used to amplify the long non-coding RNA *AT1G07887* and *UBIQUITIN10*, respectively. Primer pair efficiencies were tested prior to the analysis. For analysis, the ΔΔCt method was applied. Relative expression levels were inferred as $2^{\wedge}-\Delta Ct$ values of biological replicates. The significance ($P<0.001$) of differences between the wild type and *rh17-1/RH17* was tested with two-tailed, unpaired Student's *t*-test.

References
Adamski, N. M., Anastasiou, E., Eriksson, S., O'Neill, C. M. and Lenhard, M. (2009). Local maternal control of seed size by KLUH/CYP78A5-dependent growth signaling. *Proc. Natl. Acad. Sci. USA* **106**, 20115-20120. doi:10.1073/pnas.0907024106

Albert, B., Kos-Braun, I. C., Henras, A. K., Dez, C., Rueda, M. P., Zhang, X., Gadal, O., Kos, M. and Shore, D. (2019). A ribosome assembly stress response regulates transcription to maintain proteome homeostasis. *eLife* **8**, e45002. doi:10.7554/eLife.45002

Albertini, E., Barcaccia, G., Carman, J. G. and Pupilli, F. (2019). Did apomixis evolve from sex or was it the other way around? *J. Exp. Bot.* **70**, 2951-2964. doi:10.1093/jxb/erz109

Alexa A, R. J. (2019). topGO: Enrichment Analysis for Gene Ontology. R package version 2.38.1.

Anderson, L. E. (1954). Hoyer's solution as a rapid permanent mounting medium for bryophytes. *Bryologist* **57**, 242-244. doi:10.1639/0007-2745(1954)57[242: HSAARP]2.0.CO;2

Barcaccia, G. and Albertini, E. (2013). Apomixis in plant reproduction: a novel perspective on an old dilemma. *Plant Reprod.* **26**, 159-179. doi:10.1007/s00497-013-0222-y

Batista, R. A., Figueiredo, D. D., Santos-González, J. and Köhler, C. (2019). Auxin regulates endosperm cellularization in Arabidopsis. *Genes Dev.* **33**, 466-476. doi:10.1101/gad.316554.118

Bemer, M., Heijmans, K., Airoldi, C., Davies, B. and Angenent, G. C. (2010). An atlas of type I MADS box gene expression during female gametophyte and seed development in Arabidopsis. *Plant Physiol.* **154**, 287-300. doi:10.1104/pp.110.160770

Bicknell, R. A. and Koltunow, A. M. (2004). Understanding apomixis: recent advances and remaining conundrums. *Plant Cell* **16**, S228-S245. doi:10.1105/tpc.017921

Borg, M., Brownfield, L. and Twell, D. (2009). Male gametophyte development: a molecular perspective. *J. Exp. Bot.* **60**, 1465-1478. doi:10.1093/jxb/ern355

Brockdorff, N. (2013). Noncoding RNA and Polycomb recruitment. *RNA* **19**, 429-442. doi:10.1261/rna.037598.112

Bui, M., Lim, N., Sijacic, P. and Liu, Z. (2011). Leunig_homolog and leunig regulate seed mucilage extrusion in Arabidopsis. *J. Integr. Plant Biol.* **53**, 399-408. doi:10.1111/j.1744-7909.2011.01036.x

Cao, L., Wang, S., Venglat, P., Zhao, L., Cheng, Y., Ye, S., Qin, Y., Datla, R., Zhou, Y. and Wang, H. (2018). Arabidopsis ICK/KRP cyclin-dependent kinase inhibitors function to ensure the formation of one megaspore mother cell and one functional megaspore per ovule. *PLoS Genet.* **14**, e1007230. doi:10.1371/journal.pgen.1007230

Carman, J. G. (1997). Asynchronous expression of duplicate genes in angiosperms may cause apomixis, bispory, tetraspory, and polyembryony. *Biol. J. Linn. Soc.* **61**, 51-94. doi:10.1111/j.1095-8312.1997.tb01778.x

Carman, J. G., Mateo de Arias, M., Gao, L., Zhao, X., Kowallis, B. M., Sherwood, D. A., Srivastava, M. K., Dwivedi, K. K., Price, B. J., Watts, L. et al. (2019). Apospory and diplospory in diploid Boechera (Brassicaceae) may facilitate speciation by recombination-driven apomixis-to-sex reversals. *Front. Plant Sci.* **10**, 724. doi:10.3389/fpls.2019.00724

Castellano-Pozo, M., García-Muse, T. and Aguilera, A. (2012). R-loops cause replication impairment and genome instability during meiosis. *EMBO Rep.* **13**, 923-929. doi:10.1038/embor.2012.119

Chen, Q., Lai, H., Hurtado, J., Stahnke, J., Leuzinger, K. and Dent, M. (2013). Agroinfiltration as an effective and scalable strategy of gene delivery for production of pharmaceutical proteins. *Adv. Tech. Biol. Med.* **1**, 103. doi:10.4172/2379-1764.1000103

Chi, W., He, B., Mao, J., Li, Q., Ma, J., Ji, D., Zou, M. and Zhang, L. (2012). The function of RH22, a DEAD RNA helicase, in the biogenesis of the 50S ribosomal subunits of Arabidopsis chloroplasts. *Plant Physiol.* **158**, 693-707. doi:10.1104/pp.111.186775

Conner, J. A. and Ozias-Akins, P. (2017). Apomixis: engineering the ability to harness hybrid vigor in crop plants. *Methods Mol. Biol.* **1669**, 17-34. doi:10.1007/978-1-4939-7286-9_2

Dalla Venezia, N., Vincent, A., Marcel, V., Catez, F. and Diaz, J.-J. (2019). Emerging role of eukaryote ribosomes in translational control. *Int. J. Mol. Sci.* **20**, 1226. doi:10.3390/ijms20051226

De Muyt, A., Zhang, L., Piolot, T., Kleckner, N., Espagne, E. and Zickler, D. (2014). E3 ligase Hei10: a multifaceted structure-based signaling molecule with roles within and beyond meiosis. *Genes Dev.* **28**, 1111-1123. doi:10.1101/gad.240408.114

Dobin, A., Davis, C. A., Schlesinger, F., Drenkow, J., Zaleski, C., Jha, S., Batut, P., Chaisson, M. and Gingeras, T. R. (2013). STAR: ultrafast universal RNA-seq aligner. *Bioinformatics* **29**, 15-21. doi:10.1093/bioinformatics/bts635

Eckardt, N. A. (2003). Patterns of gene expression in apomixis. *Plant Cell* **15**, 1499-1501. doi:10.1105/tpc.150710

Figueiredo, D. D. and Köhler, C. (2018). Auxin: a molecular trigger of seed development. *Genes Dev.* **32**, 479-490. doi:10.1101/gad.312546.118

Figueiredo, D. D., Batista, R. A., Roszak, P. J., Hennig, L. and Köhler, C. (2016). Auxin production in the endosperm drives seed coat development in Arabidopsis. *eLife* **5**, e20542. doi:10.7554/eLife.20542

Grossniklaus, U. and Schneitz, K. (1998). The molecular and genetic basis of ovule and megagametophyte development. *Semin. Cell Dev. Biol.* **9**, 227-238. doi:10.1006/scdb.1997.0214

Hand, M. L. and Koltunow, A. M. G. (2014). The genetic control of apomixis: asexual seed formation. *Genetics* **197**, 441-450. doi:10.1534/genetics.114.163105

Honys, D., Reňák, D., Feciková, J., Jedelský, P. L., Nebesářová, J., Dobrev, P. and Čapková, V. (2009). Cytoskeleton-associated large RNP complexes in tobacco male gametophyte (EPPs) are associated with ribosomes and are involved in protein synthesis, processing, and localization. *J. Proteome Res.* **8**, 2015-2031. doi:10.1021/pr8009897

Hove, C. A., Lu, K.-J. and Weijers, D. (2015). Building a plant: cell fate specification in the early Arabidopsis embryo. *Development* **142**, 420-430. doi:10.1242/dev.111500

Hsu, Y.-F., Chen, Y.-C., Hsiao, Y.-C., Wang, B.-J., Lin, S.-Y., Cheng, W.-H., Jauh, G.-Y., Harada, J. J. and Wang, C.-S. (2014). AtRH57, a DEAD-box RNA helicase, is involved in feedback inhibition of glucose-mediated abscisic acid accumulation during seedling development and additively affects pre-ribosomal RNA processing with high glucose. *Plant J.* **77**, 119-135. doi:10.1111/tpj.12371

Huang, C.-K., Huang, L.-F., Huang, J.-J., Wu, S.-J., Yeh, C.-H. and Lu, C.-A. (2010). A DEAD-box protein, AtRH36, is essential for female gametophyte development and is involved in rRNA biogenesis in Arabidopsis. *Plant Cell Physiol.* **51**, 694-706. doi:10.1093/pcp/pcq045

Khanday, I., Skinner, D., Yang, B., Mercier, R. and Sundaresan, V. (2019). A male-expressed rice embryogenic trigger redirected for asexual propagation through seeds. *Nature* **565**, 91-95. doi:10.1038/s41586-018-0785-8

Kiefer, M., Nauerth, B. H., Volkert, C., Ibberson, D., Loreth, A. and Schmidt, A. (2020). Gene function rather than reproductive mode drives the evolution of RNA helicases in sexual and apomictic Boechera. *Genome Biol. Evol.* **12**, 656-673. doi:10.1093/gbe/evaa078

Kishore, K. (2014). Polyembryony. In *Reproductive Biology of Plants* (ed. K. G. Ramawat, J.-M. Merillon and K. R. Shivanna), pp. 355-370. CRC Press.

Koltunow, A. M. and Grossniklaus, U. (2003). Apomixis: a developmental perspective. *Annu. Rev. Plant Biol.* **54**, 547-574. doi:10.1146/annurev.arplant.54.110901.160842

Kong, J., Lau, S. and Jürgens, G. (2015). Twin plants from supernumerary egg cells in Arabidopsis. *Curr. Biol.* **25**, 225-230. doi:10.1016/j.cub.2014.11.021

Kotliński, M., Knizewski, L., Muszewska, A., Rutowicz, K., Lirski, M., Schmidt, A., Baroux, C., Ginalski, K. and Jerzmanowski, A. (2017). Phylogeny-based systematization of Arabidopsis proteins with histone H1 globular domain. *Plant Physiol.* **174**, 27-34. doi:10.1104/pp.16.00214

Lampropoulos, A., Sutikovic, Z., Wenzl, C., Maegele, I., Lohmann, J. U. and Forner, J. (2013). GreenGate - a novel, versatile, and efficient cloning system for plant transgenesis. *PLoS ONE* **8**, e83043. doi:10.1371/journal.pone.0083043

Lawit, S. J., Chamberlin, M. A., Agee, A., Caswell, E. S. and Albertsen, M. C. (2013). Transgenic manipulation of plant embryo sacs tracked through cell-type-specific fluorescent markers: cell labeling, cell ablation, and adventitious embryos. *Plant Reprod.* **26**, 125-137. doi:10.1007/s00497-013-0215-x

Lee, K.-H., Park, J., Williams, D. S., Xiong, Y., Hwang, I. and Kang, B.-H. (2013). Defective chloroplast development inhibits maintenance of normal levels of abscisic acid in a mutant of the Arabidopsis RH3 DEAD-box protein during early post-germination growth. *Plant J.* **73**, 720-732. doi:10.1111/tpj.12055

Liu, Y. and Imai, R. (2018). Function of plant DExD/H-Box RNA helicases associated with ribosomal RNA biogenesis. *Front. Plant Sci.* **9**, 125. doi:10.3389/fpls.2018.00125

Liu, M., Shi, D.-Q., Yuan, L., Liu, J. and Yang, W.-C. (2010). *SLOW WALKER3*, encoding a putative DEAD-box RNA helicase, is essential for female gametogenesis in *Arabidopsis. J. Integr. Plant Biol.* **52**, 817-828. doi:10.1111/j.1744-7909.2010.00972.x

Lora, J., Yang, X. and Tucker, M. R. (2019). Establishing a framework for female germline initiation in the plant ovule. *J. Exp. Bot.* **70**, 2937-2949. doi:10.1093/jxb/erz212

Lucas, M., Kenobi, K., von Wangenheim, D., Voβ, U., Swarup, K., De Smet, I., Van Damme, D., Lawrence, T., Péret, B., Moscardi, E. et al. (2013). Lateral root morphogenesis is dependent on the mechanical properties of the overlaying tissues. *Proc. Natl. Acad. Sci. USA* **110**, 5229-5234. doi:10.1073/pnas.1210807110

Marimuthu, M. P. A., Jolivet, S., Ravi, M., Pereira, L., Davda, J. N., Cromer, L., Wang, L., Nogue, F., Chan, S. W. L., Siddiqi, I. et al. (2011). Synthetic clonal reproduction through seeds. *Science* **331**, 876. doi:10.1126/science.1199682

Martin, M. (2011). CUTADAPT removes adapter sequences from high-throughput sequencing reads. *EMBnet.J.* **17**, 10-12. doi:10.14806/ej.17.1.200

Martin, R., Straub, A. U., Doebele, C. and Bohnsack, M. T. (2013). DExD/H-box RNA helicases in ribosome biogenesis. *RNA Biol.* **10**, 4-18. doi:10.4161/rna.21879

Maruyama, D., Hamamura, Y., Takeuchi, H., Susaki, D., Nishimaki, M., Kurihara, D., Kasahara, R. D. and Higashiyama, T. (2013). Independent control by each female gamete prevents the attraction of multiple pollen tubes. *Dev. Cell* **25**, 317-323. doi:10.1016/j.devcel.2013.03.013

Maruyama, D., Higashiyama, T., Endo, T. and Nishikawa, S.-I. (2020). Fertilization-coupled sperm nuclear fusion is required for normal endosperm nuclear proliferation. *Plant Cell Physiol.* **61**, 29-40. doi:10.1093/pcp/pcz158

Meinke, D. W. (2020). Genome-wide identification of *EMBRYO-DEFECTIVE* (*EMB*) genes required for growth and development in Arabidopsis. *New Phytol.* **226**, 306-325. doi:10.1111/nph.16071

Mendes, M. A., Petrella, R., Cucinotta, M., Vignati, E., Gatti, S., Pinto, S. C., Bird, D. C., Gregis, V., Dickinson, H., Tucker, M. R. et al. (2020). The RNA-dependent DNA methylation pathway is required to restrict *SPOROCYTELESS/NOZZLE* expression to specify a single female germ cell precursor in Arabidopsis. *Development* **147**, dev194274. doi:10.1242/dev.194274

Merchante, C., Stepanova, A. N. and Alonso, J. M. (2017). Translation regulation in plants: an interesting past, an exciting present and a promising future. *Plant J.* **90**, 628-653. doi:10.1111/tpj.13520

Mingam, A., Toffano-Nioche, C., Brunaud, V., Boudet, N., Kreis, M. and Lecharny, A. (2004). DEAD-box RNA helicases in Arabidopsis thaliana: establishing a link between quantitative expression, gene structure and evolution of a family of genes. *Plant Biotechnol. J.* **2**, 401-415. doi:10.1111/j.1467-7652.2004.00084.x

Mizzotti, C., Ezquer, I., Paolo, D., Rueda-Romero, P., Guerra, R. F., Battaglia, R., Rogachev, I., Aharoni, A., Kater, M. M., Caporali, E. et al. (2014). SEEDSTICK is a master regulator of development and metabolism in the Arabidopsis seed coat. *PLoS Genet.* **10**, e1004856. doi:10.1371/journal.pgen.1004856

Möller, B. and Weijers, D. (2009). Auxin control of embryo patterning. *Cold Spring Harb. Perspect Biol.* **1**, a001545. doi:10.1101/cshperspect.a001545

Mozgova, I., Köhler, C. and Hennig, L. (2015). Keeping the gate closed: functions of the Polycomb repressive complex PRC2 in development. *Plant J.* **83**, 121-132. doi:10.1111/tpj.12828

Musielak, T. J., Schenkel, L., Kolb, M., Henschen, A. and Bayer, M. (2015). A simple and versatile cell wall staining protocol to study plant reproduction. *Plant Reprod.* **28**, 161-169. doi:10.1007/s00497-015-0267-1

Nair, L., Chung, H. and Basu, U. (2020). Regulation of long non-coding RNAs and genome dynamics by the RNA surveillance machinery. *Nat. Rev. Mol. Cell Biol.* **21**, 123-136. doi:10.1038/s41580-019-0209-0

Nakajima, K. (2018). Be my baby: patterning toward plant germ cells. *Curr. Opin. Plant Biol.* **41**, 110-115. doi:10.1016/j.pbi.2017.11.002

Nguyen, L. V., Seok, H.-Y., Woo, D.-H., Lee, S.-Y. and Moon, Y.-H. (2018). Overexpression of the DEAD-Box RNA helicase gene AtRH17 confers tolerance to salt stress in Arabidopsis. *Int. J. Mol. Sci.* **19**, 3777. doi:10.3390/ijms19123777

Nishimura, K., Ashida, H., Ogawa, T. and Yokota, A. (2010). A DEAD box protein is required for formation of a hidden break in Arabidopsis chloroplast 23S rRNA. *Plant J.* **63**, 766-777. doi:10.1111/j.1365-313X.2010.04276.x

Olmedo-Monfil, V., Durán-Figueroa, N., Arteaga-Vázquez, M., Demesa-Arévalo, E., Autran, D., Grimanelli, D., Slotkin, R. K., Martienssen, R. A. and Vielle-Calzada, J.-P. (2010). Control of female gamete formation by a small RNA pathway in Arabidopsis. *Nature* **464**, 628-632. doi:10.1038/nature08828

Orozco-Arroyo, G., Paolo, D., Ezquer, I. and Colombo, L. (2015). Networks controlling seed size in Arabidopsis. *Plant Reprod.* **28**, 17-32. doi:10.1007/s00497-015-0255-5

Owttrim, G. W. (2013). RNA helicases: diverse roles in prokaryotic response to abiotic stress. *RNA Biol.* **10**, 96-110. doi:10.4161/rna.22638

Paieri, F., Tadini, L., Manavski, N., Kleine, T., Ferrari, R., Morandini, P., Pesaresi, P., Meurer, J. and Leister, D. (2018). The DEAD-box RNA Helicase RH50 Is a 23S-4.5S rRNA maturation factor that functionally overlaps with the plastid signaling factor GUN1. *Plant Physiol.* **176**, 634-648. doi:10.1104/pp.17.01545

Palm, D., Streit, D., Shanmugam, T., Weis, B. L., Ruprecht, M., Simm, S. and Schleiff, E. (2019). Plant-specific ribosome biogenesis factors in Arabidopsis thaliana with essential function in rRNA processing. *Nucleic Acids Res.* **47**, 1880-1895. doi:10.1093/nar/gky1261

Peterson, R., Slovin, J. P. and Chen, C. (2010). A simplified method for differential staining of aborted and non-aborted pollen grains. *Int. J. Plant Biol.* **1**, e13. doi:10.4081/pb.2010.e13

Pillot, M., Baroux, C., Vazquez, M. A., Autran, D., Leblanc, O., Vielle-Calzada, J. P., Grossniklaus, U. and Grimanelli, D. (2010). Embryo and endosperm inherit distinct chromatin and transcriptional states from the female gametes in Arabidopsis. *Plant Cell* **22**, 307-320. doi:10.1105/tpc.109.071647

Pinto, S. C., Mendes, M. A., Coimbra, S. and Tucker, M. R. (2019). Revisiting the female germline and its expanding toolbox. *Trends Plant Sci.* **24**, 455-467. doi:10.1016/j.tplants.2019.02.003

Prusicki, M. A., Keizer, E. M., van Rosmalen, R. P., Komaki, S., Seifert, F., Müller, K., Wijnker, E., Fleck, C. and Schnittger, A. (2019). Live cell imaging of meiosis in Arabidopsis thaliana. *eLife* **8**, e42834. doi:10.7554/eLife.42834

Robert, H. S., Crhak Khaitova, L., Mroue, S. and Benková, E. (2015). The importance of localized auxin production for morphogenesis of reproductive organs and embryos in Arabidopsis. *J. Exp. Bot.* **66**, 5029-5042. doi:10.1093/jxb/erv256

Robinson, M. D., McCarthy, D. J. and Smyth, G. K. (2009). edgeR: a Bioconductor package for differential expression analysis of digital gene expression data. *Bioinformatics* **26**, 139-140. doi:10.1093/bioinformatics/btp616

Rosado, A., Sohn, E. J., Drakakaki, G., Pan, S., Swidergal, A., Xiong, Y., Kang, B.-H., Bressan, R. A. and Raikhel, N. V. (2010). Auxin-mediated

ribosomal biogenesis regulates vacuolar trafficking in Arabidopsis. *Plant Cell* **22**, 143-158. doi:10.1105/tpc.109.068320

Rosado, A., Li, R., van de Ven, W., Hsu, E. and Raikhel, N. V. (2012). Arabidopsis ribosomal proteins control developmental programs through translational regulation of auxin response factors. *Proc. Natl. Acad. Sc. USA* **109**, 19537-19544. doi:10.1073/pnas.1214774109

Rotman, N., Durbarry, A., Wardle, A., Yang, W. C., Chaboud, A., Faure, J.-E., Berger, F. and Twell, D. (2005). A novel class of MYB factors controls sperm-cell formation in plants. *Curr. Biol.* **15**, 244-248. doi:10.1016/j.cub.2005.01.013

Santos-Pereira, J. M. and Aguilera, A. (2015). R loops: New modulators of genome dynamics and function. *Nat. Rev. Genet.* **16**, 583-597. doi:10.1038/nrg3961

Scheben, A. and Hojsgaard, D. (2020). Can we use gene-editing to induce apomixis in sexual plants? *Genes* **11**, 781. doi:10.3390/genes11070781

Schmid, M. W. (2017). RNA-seq data analysis protocol: combining in-house and publicly available data. In *Plant Germline Development: Methods and Protocols* (ed. A. Schmidt), pp. 309-335. New York, New York, NY: Springer.

Schmid, M. W., Schmidt, A. and Grossniklaus, U. (2015). The female gametophyte: an emerging model for cell type-specific systems biology in plant development. *Front. Plant Sci.* **6**, 907. doi:10.3389/fpls.2015.00907

Schmidt, A. (2020). Controlling apomixis: shared features and distinct characteristics of gene regulation. *Genes* **11**, 329. doi:10.3390/genes11030329

Schmidt, A., Wuest, S. E., Vijverberg, K., Baroux, C., Kleen, D. and Grossniklaus, U. (2011). Transcriptome analysis of the Arabidopsis megaspore mother cell uncovers the importance of RNA helicases for plant germline development. *PLoS Biol.* **9**, e1001155. doi:10.1371/journal.pbio.1001155

Schmidt, A., Schmid, M. W., Klostermeier, U. C., Qi, W., Guthörl, D., Sailer, C., Waller, M., Rosenstiel, P. and Grossniklaus, U. (2014). Apomictic and sexual germline development differ with respect to cell cycle, transcriptional, hormonal and epigenetic regulation. *PLoS Genet.* **10**, e1004476. doi:10.1371/journal.pgen.1004476

Schmidt, A., Schmid, M. W. and Grossniklaus, U. (2015). Plant germline formation: common concepts and developmental flexibility in sexual and asexual reproduction. *Development* **142**, 229-241. doi:10.1242/dev.102103

She, W. (2014). Chromatin reprogramming during the somatic-to-reproductive cell fate transition in plants. *PhD thesis*. University of Zurich, Zurich, Switzerland.

Shirzadi, R., Andersen, E. D., Bjerkan, K. N., Gloeckle, B. M., Heese, M., Ungru, A., Winge, P., Koncz, C., Aalen, R. B., Schnittger, A. et al. (2011). Genome-wide transcript profiling of endosperm without paternal contribution identifies parent-of-origin–dependent regulation of AGAMOUS-LIKE36. *PLoS Genet.* **7**, e1001303. doi:10.1371/journal.pgen.1001303

Steffen, J. G., Kang, I.-H., Portereiko, M. F., Lloyd, A. and Drews, G. N. (2008). AGL61 interacts with AGL80 and is required for central cell development in Arabidopsis. *Plant Physiol.* **148**, 259-268. doi:10.1104/pp.108.119404

Su, Z., Wang, N., Hou, Z., Li, B., Li, D., Liu, Y., Cai, H., Qin, Y. and Chen, X. (2020). Regulation of female germline specification via small RNA mobility in Arabidopsis. *Plant Cell* **32**, 2842-2854. doi:10.1105/tpc.20.00126

Sun, B., Looi, L.-S., Guo, S., He, Z., Gan, E.-S., Huang, J., Xu, Y., Wee, W.-Y. and Ito, T. (2014). Timing mechanism dependent on cell division is invoked by Polycomb eviction in plant stem cells. *Science* **343**, 1248559. doi:10.1126/science.1248559

Tucker, M. R., Okada, T., Hu, Y., Scholefield, A., Taylor, J. M. and Koltunow, A. M. G. (2012). Somatic small RNA pathways promote the mitotic events of megagametogenesis during female reproductive development in Arabidopsis. *Development* **139**, 1399-1404. doi:10.1242/dev.075390

Vernon, D. M. and Meinke, D. W. (1994). Embryogenic transformation of the suspensor in *twin*, a polyembryonic mutant of Arabidopsis. *Dev. Biol.* **165**, 566-573. doi:10.1006/dbio.1994.1276

Waadt, R., Krebs, M., Kudla, J. and Schumacher, K. (2017). Multiparameter imaging of calcium and abscisic acid and high-resolution quantitative calcium measurements using R-GECO1-mTurquoise in Arabidopsis. *New Phytol.* **216**, 303-320. doi:10.1111/nph.14706

Wickham, H. (2016). *ggplot2: Elegant Graphics for Data Analysis*. New York: Springer-Verlag.

Wuest, S. E., Vijverberg, K., Schmidt, A., Weiss, M., Gheyselinck, J., Lohr, M., Wellmer, F., Rahnenführer, J., von Mering, C. and Grossniklaus, U. (2010). Arabidopsis female gametophyte gene expression map reveals similarities between plant and animal gametes. *Curr. Biol.* **20**, 506-512. doi:10.1016/j.cub.2010.01.051

Xu, J., Liu, C., Li, M., Hu, J., Zhu, L., Zeng, D., Yang, Y., Peng, Y., Ruan, B., Guo, L. et al. (2015). A rice DEAD-box RNA helicase protein, OsRH17, suppresses 16S ribosomal RNA maturation in Escherichia coli. *Gene* **555**, 318-328. doi:10.1016/j.gene.2014.11.025

Xu, W., Li, K., Li, S., Hou, Q., Zhang, Y., Liu, K. and Sun, Q. (2020). The R-loop atlas of Arabidopsis development and responses to environmental stimuli. *Plant Cell* **32**, 888-903. doi:10.1105/tpc.19.00802

Xuan, L., Wang, Z. and Jiang, L. (2014). Vanillin assay of Arabidopsis seeds for proanthocyanidins. *Bio-Protocol* **4**, e1309. doi:10.21769/BioProtoc.1309

Yao, X., Feng, H., Yu, Y., Dong, A. and Shen, W.-H. (2013). SDG2-mediated H3K4 methylation is required for proper arabidopsis root growth and development. *PLoS ONE* **8**, e56537. doi:10.1371/journal.pone.0056537

Zhang, Y., Glazebrook, J. and Li, X. (2007). Identification of components in disease-resistance signaling in Arabidopsis by map-based cloning. *Methods Mol. Biol.* **354**, 69-78.

Zhao, X., Bramsiepe, J., Van Durme, M., Komaki, S., Prusicki, M. A., Maruyama, D., Forner, J., Medzihradszky, A., Wijnker, E., Harashima, H. et al. (2017). Retinoblastoma Related1 mediates germline entry in Arabidopsis. *Science* **356**, eaaf6532. doi:10.1126/science.aaf6532

Zhao, L., Cai, H., Su, Z., Wang, L., Huang, X., Zhang, M., Chen, P., Dai, X., Zhao, H., Palanivelu, R. et al. (2018). KLU suppresses megasporocyte cell fate through SWR1-mediated activation of WRKY28 expression in Arabidopsis. *Proc. Natl. Acad. Sc. USA* **115**, E526-E535. doi:10.1073/pnas.1716054115

Ziolkowski, P. A., Underwood, C. J., Lambing, C., Martinez-Garcia, M., Lawrence, E. J., Ziolkowska, L., Griffin, C., Choi, K., Franklin, F. C. H., Martienssen, R. A. et al. (2017). Natural variation and dosage of the HEI10 meiotic E3 ligase control Arabidopsis crossover recombination. *Genes Dev.* **31**, 306-317. doi:10.1101/gad.295501.116

Zühl, L., Volkert, C., Ibberson, D. and Schmidt, A. (2019). Differential activity of F-box genes and E3 ligases distinguishes sexual versus apomictic germline specification in Boechera. *J. Exp. Bot.* **70**, 5643-5657. doi:10.1093/jxb/erz323
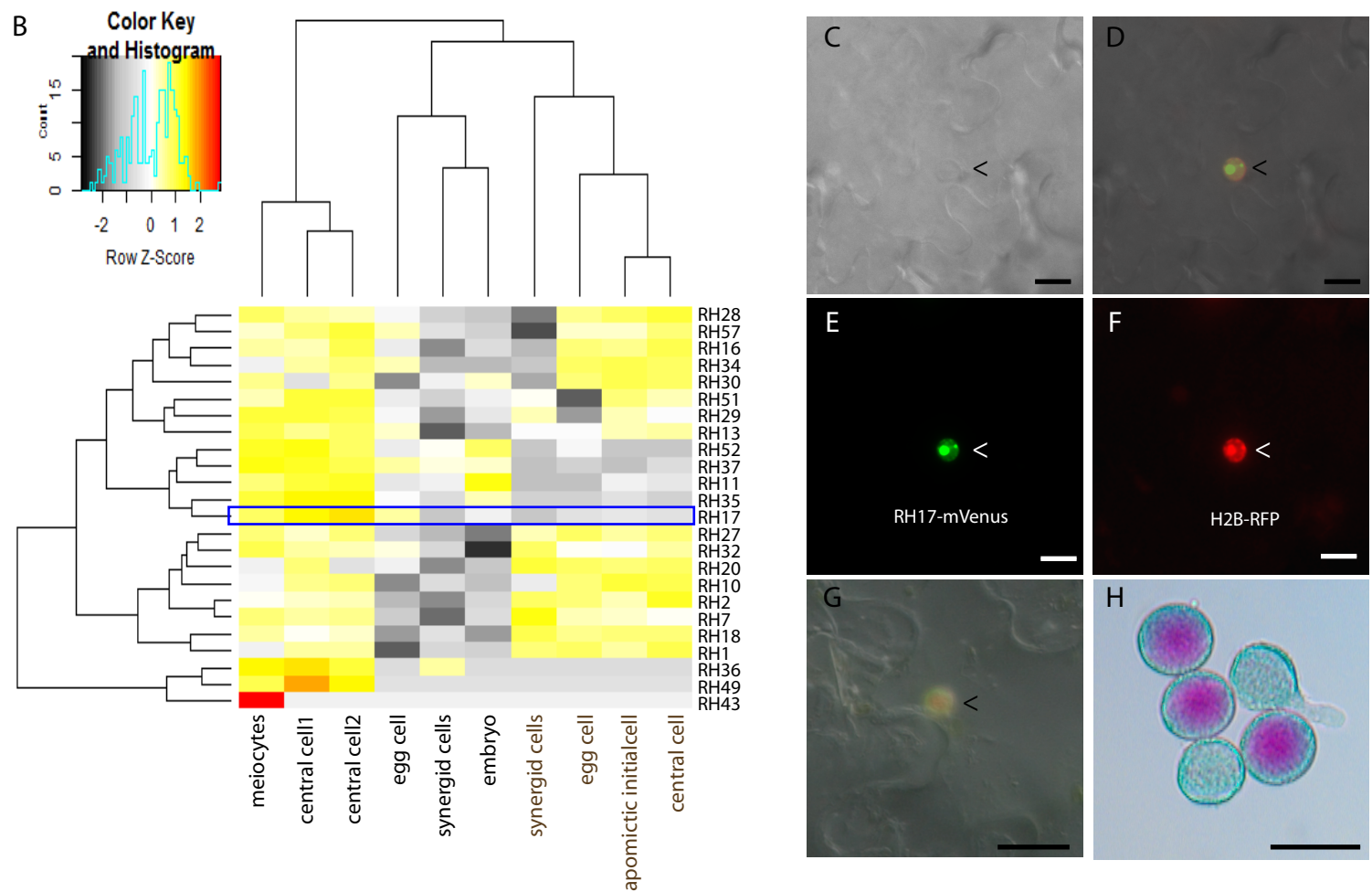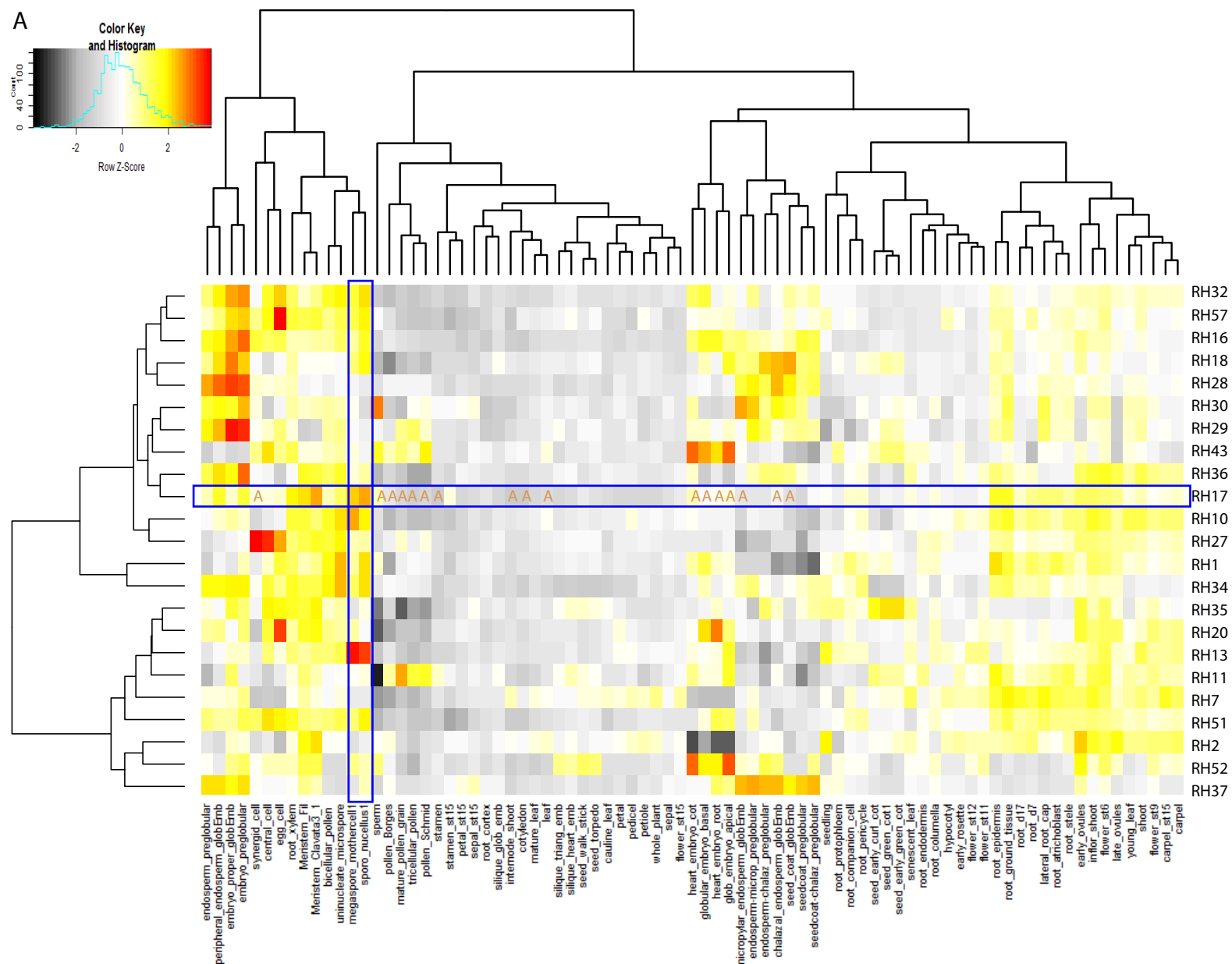
DEVELOPMENT

Fig. S1. Heatmap of expression, subcellular localization, and pollen viability. (A,B) Analysis of expression of DEAD-box RNA helicases with homologies to yeast and human ribosomal binding factors (Liu and Imai, 2018). (A) Heatmap of log2-transformed mean expression values in a total of 74 cell types and tissues in Arabidopsis as used in (Kotliński et al., 2017). (B) Heatmap of normalized log2-transformed read counts from reproductive cell and tissue types of Arabidopsis or *Boechera gunnisoniana* as reported in (Schmidt et al., 2014). (A,B) Hierarchical clustering of genes and samples was based on euclidean distance and agglomerative hierarchical clustering. Red denotes high expression and black low expression. Blue boxes indicate the row of *RH17* expression values and the columns of the megaspore mother cell and surrounding sporophytic nucellus tissues. "A" indicates the absence in the majority of biological replicates evaluated as previously described (Schmidt et al., 2011). (C-G) Subcellular localization of RH17 fused to mVenus by epifluorescence microscopy after transient expression in *Nicotiana benthamiana* leaves under the control of the Arabidopsis *UBIQUTIN10* (*UBI10*) promoter. As control for expression in the nucleus, co-transformation with a construct driving the expression of H2B-RFP under the control of the *UBI10* promoter was applied (Lucas et al., 2013). (C) Cells visualized by differential inference contrast (DIC) microscopy, (E) RH17-mVenus and (F) H2B-RFP localization in the nucleus (arrows), and (D) overlay of DIC, YFP and RFP channels. (G) Colocalization of RH17-mVenus and H2B-RFP in the nucleus (arrow). (H) Analysis of pollen viability analyzed by Alexander Staining (Ross et al., 2010) and light microscopy. Pink staining indicates viable pollen and blue staining aborted pollen. Scale bars are 20 µm.
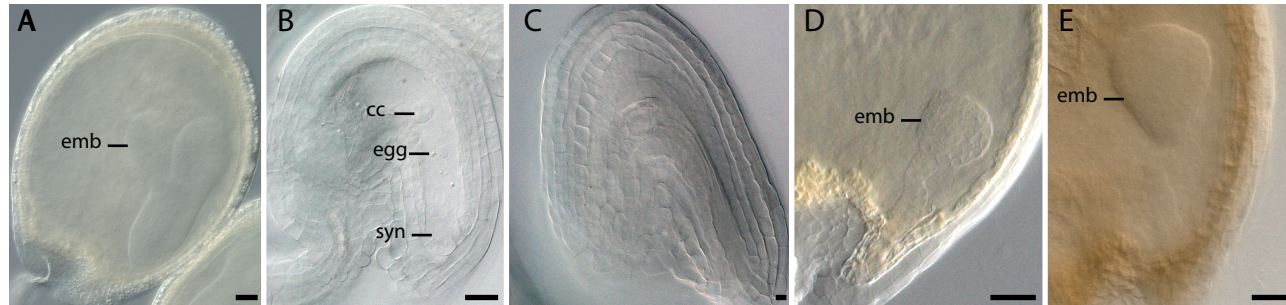
Fig. S2. Morphological investigation of ovule and seed development. (A) Seed with embryo (emb) at torpedo stage of development in the wild-type. Unfertilized or unfertile mature gametophyte (B) and over-proliferated embryo (E) in silique of *rh17-1/RH17* (egg, egg cell; cc, central cell; syn, synergids). Seed with only seed coat formed (C) and over-proliferated embryo (D) in *rh17-2/RH17*. Scale bars are 20 µm.
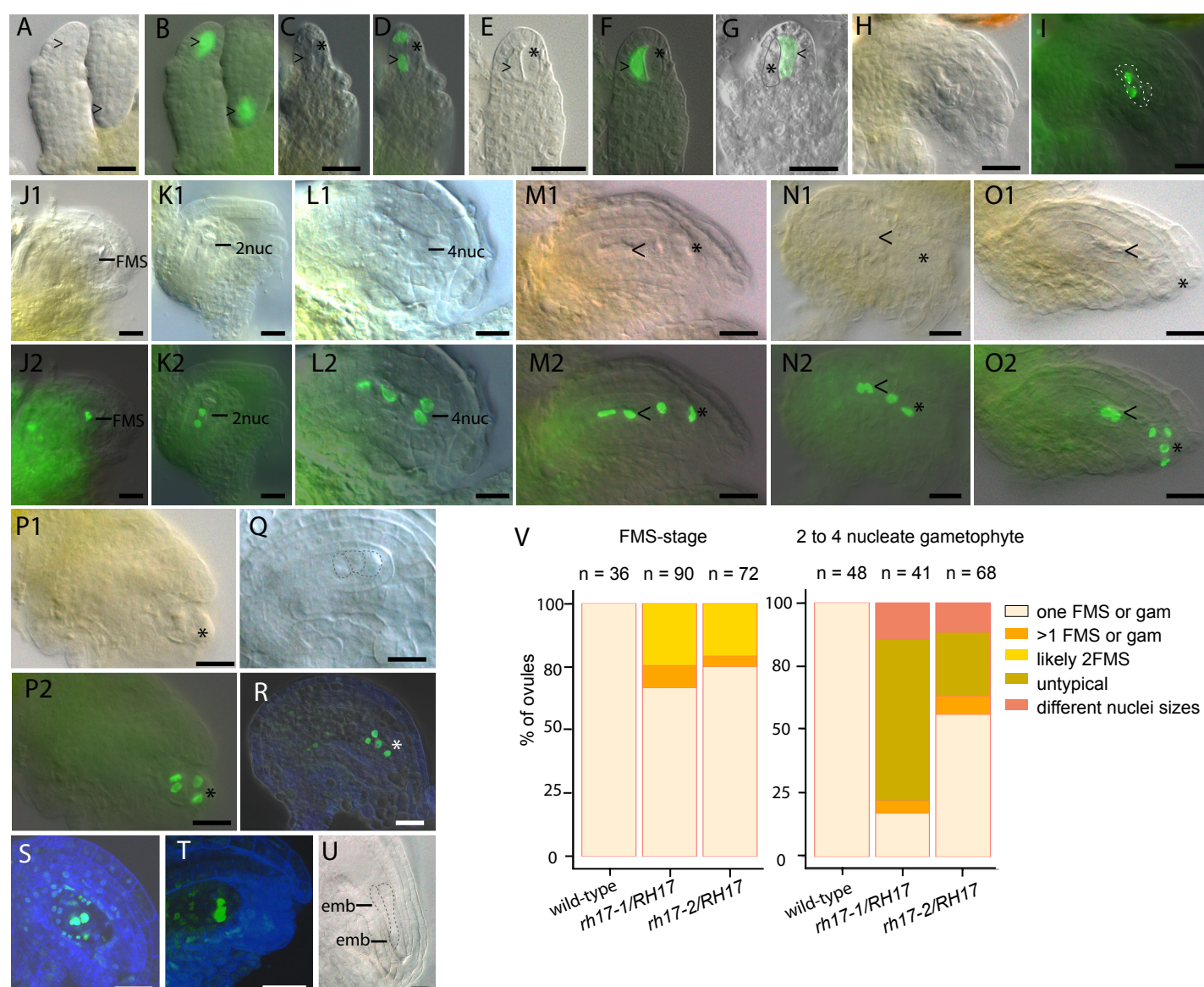
Fig. S3. Formation of more than one germline lineage per ovule. Epifluorescence microscopy (B, D, F, I, J2-O2, P2), (corresponding) DIC images (A, C, E, H, J1-O1, P1, Q, U), and laser scanning microscopy (G, R-T; blue signal: Renaissance 2200 cell-wall dye). MMCs are indicated by arrows, additionally enlarged cells are marked with a star. (A, B) Single MMCs in ovules of the pKNU::nlsYFP marker line serving as control. (C, D, G) Young ovules of rh17-1/RH17, and (E,F) rh17-2/RH17. (J-L) pAKV::H2B-YFP marker line used as control (Rotman et al., 2005). (M,O,R,S) Investigation of H2B-YFP activity driven by the AKV-promoter labelling gametophytic nuclei in rh17-1/RH17, and (N,P,T) rh17-2/RH17. Developing gametophytes are indicated by an arrow, ectopic gametophytes by a star. (S,T) Untypical positioning of nuclei likely indicates formation of two gametophytic lineages (counted as likely 2 FMS in V). (Q) Morphological investigation showing more than one FMS per ovule, and (U) two embryos in one seed in rh17-2/RH17. Scale bars are 20 μm. (V) Bar plot showing the frequencies of formation of additional gametophytic lineages, untypical numbers or positioning of gametophytic nuclei (untypical), or differences in sized of gametophytic nuclei observed based on H2B-YFP activity. Only ovules were scored in the category of more than one FMS or gametophyte when two cells were clearly distinguished. Differences in distributions of observations as compared to wild-type were confirmed for the lines carrying a mutant allele of RH17 by fisher's exact test (p < 0.001). Per genotype, data from at least 4 plants are summarized.
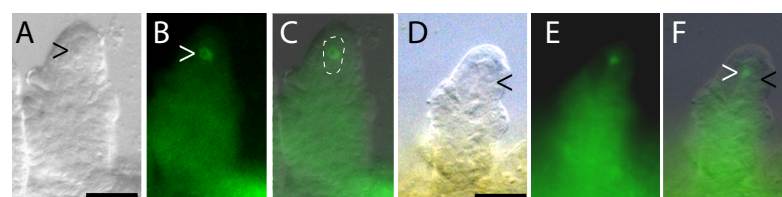

Fig. S4. REC8-mEGFP indicates meiosis of a single MMC in rh17-1/RH17. (A,D) DIC image of a MMC marked with an arrow. (B,E) Activity of PRO$_{REC8}$:REC8:mGFP (Prusicki et al., 2019) in a single MMC shown by epifluorescence microscopy, and (C,F) overlay with DIC image. Scale bars are 20 μm.
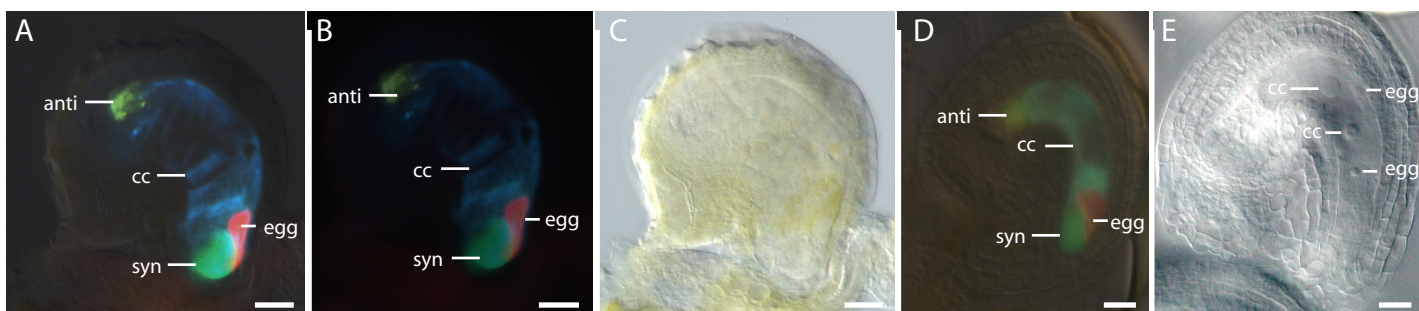
Fig. S5. Cell-type identities in mature gametophytes. Epifluorescence microscopy of representative ovules at 2-3 DAE (n = 95 and n = 62 gametophytes showing marker activity in *rh17-1/RH17* (A-C) and wild-type (D), respectively) expressing a quadruple-cassette labelling each cell of the mature gametophytewith a different fluorescent protein (Lawit et al., 2013): egg cell (egg) with DsRed, central cell (cc) with AmCyan, synergids (syn) with AcGFP, and antipodals (anti) with ZsYellow. (A,D) Overlay of DIC and fluorescent channels. (C) DIC image. (D) Clearing of mature ovule harboring two gametophytes in *rh17-2/RH17*. Scale bars are 20 µm.
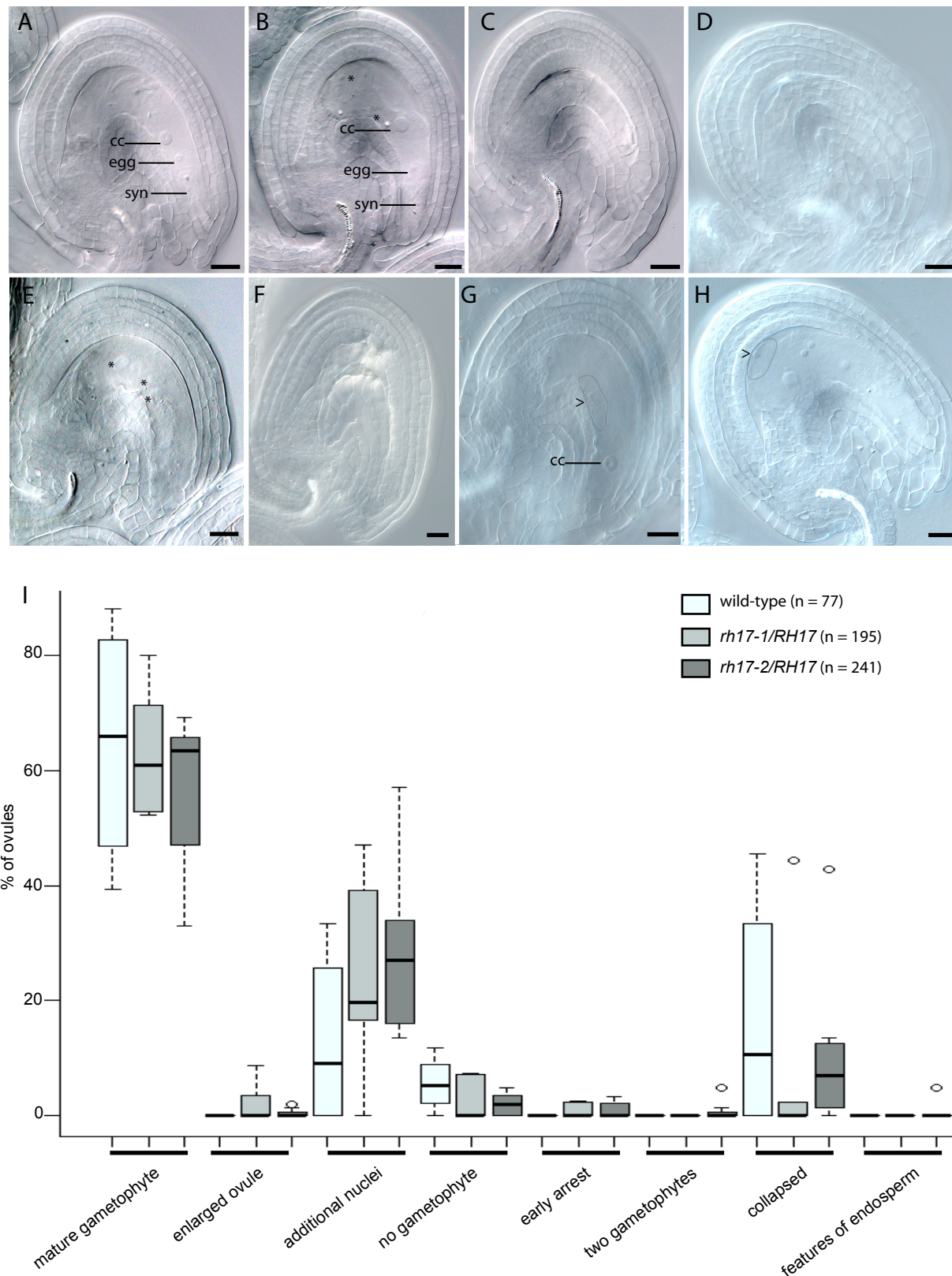
Fig. S6. Clearing of ovules at 5 DAE. (A-C) Wild-type, and (D-H) *rh17-1/RH17*. (A) Mature gametophyte. (B) Mature gametophyte with nuclei at chalazal end counted as "additional nuclei" which might represent antipodals (indicated by *). (C,D) Early developmental arrest of gametogenesis. (E) Features of autonomous endosperm (nuclei indicated by *). (F) Enlarged ovule showing features of parthenocarpy. (G,H) Ovules with additional gametophytes which have not reached maturity (indicated by >). egg egg cell, cc central cell, syn synergids; scale bars are 20 µm. (I) Box and whiskers plot summarizing observations for wild-type, *rh17-1/RH17*, and *rh17-2/RH17*.
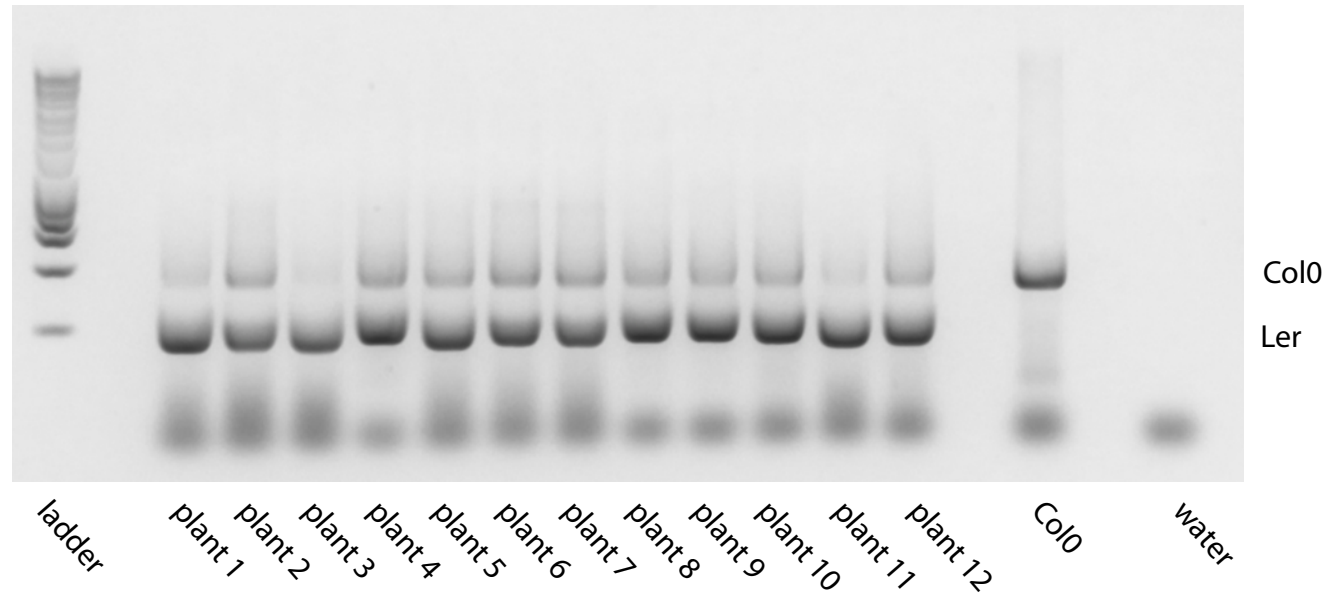
Fig. S7. Mapping approach shows hybrid identity in F1 offspring of *rh17-1/RH17* (Col-0) x L*er*.
Image of a 1% agarose gel stained with gelred showing amplification of Col-0 and Ler DNA genomic DNA from samples of 12 representative seedlings. Mapping primers T2E12F and T2E12R were used as described (Zhang et al., 2007), generating distinguishable band sizes for amplification products of each ecotype. As ladder Hyperladder I (Bioline) was used.
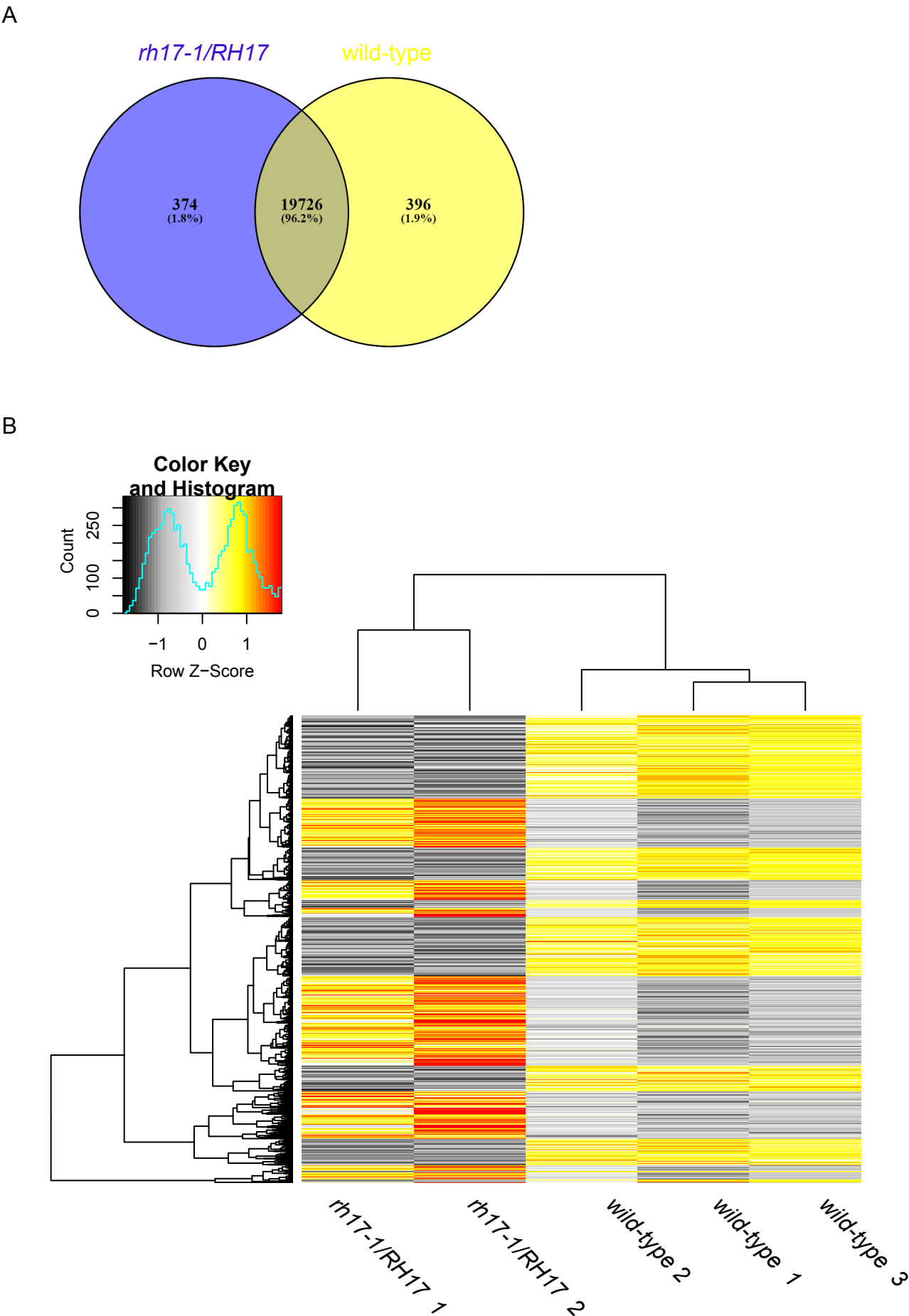
Fig. S8. Differential gene expression in ovules of *rh17-1/RH17* as compared to the wild-type at three days after emasculation. (A) Venn Diagram showing the overlap of genes expressed (> or = 10 read counts) in both samples of *rh17-1/RH17* or all samples of wild-type. (B) Heatmap based on log2-transformed TMM normalized read counts of 1'558 genes differentially expressed in samples from *rh17-1/RH17* as compared to wild-type as analyzed by EdgeR (Robinson et al., 2009). Hierarchical clustering of samples and genes was based on euclidean distance and hierarchical agglomerative clustering. Colors are scaled per row with red indicating high and black low expression.
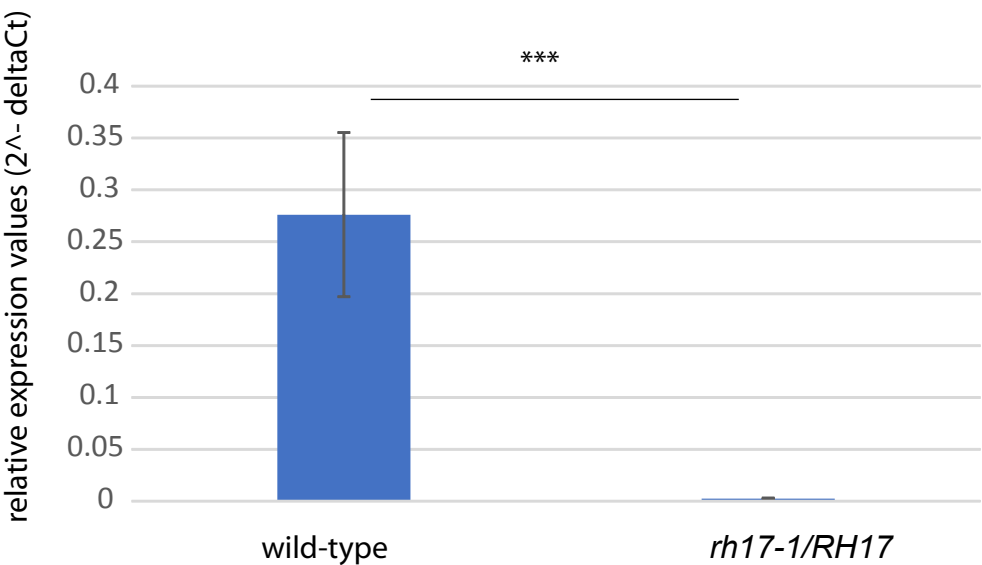
Fig. S9. Real time quantitative PCR. Relative expression levels of the long non-coding RNA AT1G07887 in ovules of wild-type as compared to *rh17-1/RH17* three days after emasculation. Shown are values averaged from three biological r eplicates and standard deviation. Significance of differences was inferred with students t-test (p<0.001).

Table S1. Summary of samples and mapping statistics. Given are for RNA-Seq libraries numbers of total raw reads and reads mapped to the A. thaliana reference genome, in addition to the numbers of genes mapped to exons using Star and counted with featureCounts (Dobin et al., 2013; Liao et al., 2014). Percentages refer to raw read numbers.

Click here to download Table S1

Table S2. TMM normalized read counts of 1'558 differentially expressed genes.

Click here to download Table S2

Table S3. Differential expression of genes in ovules of rh17-1/RH17 or wild-type at three days after emasculation.

Click here to download Table S3

Table S4. Gene ontology analysis to identify enriched biological processes.

Click here to download Table S4

Table S5. Genes represented in different enriched GO categories.

Click here to download Table S5

References

Dobin, A., Davis, C.A., Schlesinger, F., Drenkow, J., Zaleski, C., Jha, S., Batut, P., Chaisson, M., Gingeras, T.R. 2013. STAR: ultrafast universal RNA-seq aligner. *Bioinformatics (Oxford, England)* **29**, 15-21. **Kotliński, M., Knizewski, L., Muszewska, A., Rutowicz, K., Lirski, M., Schmidt, A., Baroux, C., Ginalski, K., Jerzmanowski, A.** 2017. Phylogeny-Based Systematization of Arabidopsis Proteins with Histone H1 Globular Domain. *Plant Physiol.* **174**, 27-34.

Lawit, S.J., Chamberlin, M.A., Agee, A., Caswell, E.S., Albertsen, M.C. 2013. Transgenic manipulation of plant embryo sacs tracked through cell-type-specific fluorescent markers: cell labeling, cell ablation, and adventitious embryos. *Plant Reprod.* **26**, 125-137.

Liao, Y., Smyth, G.K., Shi, W. 2014. featureCounts: an efficient general purpose program for assigning sequence reads to genomic features. *Bioinformatics* **30**, 923-930.

Liu, Y., Imai, R. 2018. Function of Plant DExD/H-Box RNA Helicases Associated with Ribosomal RNA *Biogenesis*. 9.

Lucas, M., Kenobi, K., von Wangenheim, D., Voβ, U., Swarup, K., De Smet, I., Van Damme, D., Lawrence, T., Péret, B., Moscardi, E., Barbeau, D., Godin, C., Salt, D., Guyomarc'h, S., Stelzer, E.H.K., Maizel, A., Laplaze, L., Bennett, M.J. 2013. Lateral root morphogenesis is dependent on the mechanical properties of the overlaying tissues. *Proc. Natl. Acad. Sci. U. S. A.* **110**, 5229-5234.

Prusicki, M.A., Keizer, E.M., van Rosmalen, R.P., Komaki, S., Seifert, F., Müller, K., Wijnker, E., Fleck, C., Schnittger, A. 2019. Live cell imaging of meiosis in Arabidopsis thaliana. *eLife* **8**, e42834.

Robinson, M.D., McCarthy, D.J., Smyth, G.K. 2009. edgeR: a Bioconductor package for differential expression analysis of digital gene expression data. *Bioinformatics* **26**, 139-140.

Ross, P., Slovin, J., Chen, C. 2010. A simplfied method for differential staining of aborted and non-aborted pollen grains. *Int. J. Plant Biol.* **1**, 2.

Rotman, N., Durbarry, A., Wardle, A., Yang, W.C., Chaboud, A., Faure, J.E., Berger, F., Twell, D. 2005. A novel class of MYB factors controls sperm-cell formation in plants. *Curr. Biol.* **15**, 244-248.

Schmidt, A., Schmid, M.W., Klostermeier, U.C., Qi, W., Guthorl, D., Sailer, C., Waller, M., Rosenstiel, P., Grossniklaus, U. 2014. Apomictic and sexual germline development differ with respect to cell cycle, transcriptional, hormonal and epigenetic regulation. *PLoS Genet.* **10**, e1004476.

Schmidt, A., Wuest, S.E., Vijverberg, K., Baroux, C., Kleen, D., Grossniklaus, U. 2011. Transcriptome analysis of the Arabidopsis megaspore mother cell uncovers the importance of RNA helicases for plant germline development. *PLoS Biol.* **9,** e1001155.

Zhang, Y., Glazebrook, J., Li, X. 2007. Identification of Components in Disease-Resistance Signaling in Arabidopsis by Map-Based Cloning. *Methods Mol. Biol.* **354**, 69-78.